Extension and application of the three-phase weak acid/base kinetic model to the aeration treatment of anaerobic digester liquors

EV Musvoto, GA Ekama*, MC Wentzel and RE Loewenthal
Water Research Group, Department of Civil Engineering, University of Cape Town, Rondebosch 7701, South Africa

Abstract

The kinetic model for the carbonate (inorganic carbon) system in three phases and the phosphate, short chain fatty acid and ammonia mixed weak acid/base systems in single phase, based on modelling the kinetics of the forward and reverse dissociation processes of the weak acid/base species, is extended to model the three-phase mixed weak acid/base chemical reactions in anaerobic digester liquor aeration. The kinetic reactions for ion pairing, precipitation of struvite, newberyite, amorphous calcium phosphate, calcium and magnesium carbonate and stripping of NH_3 gas are added to the model. A preliminary validation of the model was done by comparing model predictions with an equilibrium based struvite precipitation model; and equilibrium experimental results from the literature on simultaneous precipitation of calcium and magnesium carbonate and phosphate minerals. To collect data to validate the non-steady state behaviour of the model, aeration batch tests were conducted on liquor from a spent wine upflow anaerobic sludge bed (UASB) digester and a sewage sludge (SS) anaerobic digester. In the batch tests pH, Ca, Mg, Total PO_4-P (P_T), free and saline ammonia (FSA, N_T) and H_2CO_3* alkalinity (from which inorganic carbon C_T is calculated) with time were measured over 24 to 56 h. To simulate the batch test results, solubility product and ion pairing constants were obtained from the literature and the mineral precipitation and CO_2 and NH_3 gas stripping rates calibrated by minimising the error between the predicted and measured results. A very good correlation was obtained for all the measured parameters in six out of the seven batch tests, four on SS and three on UASB anaerobic digester liquors (ADL).

From the model results the masses of the different calcium and magnesium carbonate and phosphate minerals that precipitated and the CO_2 and NH_3 stripped via the gas phase could be calculated. Comparing the results from the two liquors it was found that:

- the minerals that precipitated were very similar in both, viz. in decreasing proportion of precipitate mass formed, struvite ($MgNH_4PO_4$) (82 to 89%), amorphous calcium phosphate (ACP) (5 to 15%), calcium carbonate ($CaCO_3$) (0-6%), magnesium carbonate ($MgCO_3$) (0 to 5%) and newberyite ($MgHPO_4$) (0.1 to 0.3%);
- the solubility product values for these minerals were the same in both liquors and within the range of literature values, but
- the specific precipitation rates were different;
- the rates of struvite and ACP precipitation were 9 and 2 times faster in the UASBDL than in the SSADL respectively;
- in contrast, the rate of $CaCO_3$ precipitation was 140 times faster in the SSADL than in the UASBDL;
- the rates of $MgCO_3$ and $MgHPO_4$ precipitation were approximately the same in both liquors; and
- the stripping/dissolution rates of oxygen (O_2), carbon dioxide (CO_2) and ammonia (NH_3) increased with increased aeration rate in the batch tests.

The kinetic modelling approach allows the determination of the specific precipitation rates for a number of minerals simultaneously in an integrated manner from a single batch test.

Introduction

Musvoto et al. (1997) describe the development of an integrated kinetic model to simulate the chemical-physical processes of the carbonate[1] system in three phases (solid-aqueous-gas); and the mixed water[2], carbonate, phosphate[1], short chain fatty acid (SCFA) and ammonia weak acid/base systems in single (aqueous) phase. The model was validated for the steady state (time independent) condition by comparing predicted equilibrium results with predictions from well established equilibrium chemistry based models in the literature, such as Stasoft I (Loewenthal et al., 1988) and Stasoft III (Friend and Loewenthal, 1992) for the three-phase carbonate system in pure water; and Loewenthal et al. (1989, 1991) for the single aqueous phase behaviour of the water[2], carbonate, phosphate, SCFA and ammonia mixed weak acid/base systems.

* To whom all correspondence should be addressed.
☎(021) 650-2588; fax (021) 689-7471; e-mail: ekama@eng.uct.ac.za
Received 4 September 1998; accepted in revised form 5 July 2000.

[1] *In this paper, as in the earlier paper on the same subject (Musvoto et al., 1997), the term "carbonate system" refers to the inorganic carbon system. The term "carbonate system species" refers to all the species making up the total inorganic carbon (denoted C_T), viz. H_2CO_3* comprising dissolved CO_2 and H_2CO_3, bicarbonate HCO_3^- and carbonate CO_3^{2-}, and the term "carbonate species" refers to the CO_3^{2-} species only. The same nomenclature applies to the term "phosphate system", "phosphate system species", denoted P_T, and "phosphate species".*

[2] *In aqueous single or mixed weak acid/base systems, the water always is present and acts as an additional weak acid/base system because of its dissociation to H^+ and OH^-. It is included here for completeness. In mixed weak acid/base systems, the water system is one of several weak acid/base systems that contribute to the total alkalinity and acidity mass parameters (Loewenthal et al., 1989).*

In this paper, the kinetic model is extended to describe the three-phase mixed weak acid/base reactions that occur when anaerobic digester liquors (ADL) are aerated. The resultant kinetic model, comprising the water[2], carbonate, phosphate, SCFA and ammonia weak acid/base systems, ion pairing, chemical precipitation and gas stripping is validated by comparing predictions with:

- equilibrium concentrations from:
  - an equilibrium based struvite precipitation algorithm (Loewenthal et al., 1994) coded into a computer programme called Struvite 3.1 by Loewenthal and Morrison (1997) and
  - experimental data available in the literature (Ferguson and McCarty, 1971); and
- kinetic and equilibrium data obtained from aeration batch tests on anaerobic digester liquors (ADL) from:
  - a spent wine upflow anaerobic sludge bed (UASB) digester and
  - a sewage sludge anaerobic digester.

Aeration, deliberate or inadvertent, strips CO_2 from the ADL resulting in an increase in pH; at higher pH various calcium and magnesium phosphates (and possibly carbonates) precipitate and NH_3 stripping occurs. Loss of CO_2 thus can be problematic, with magnesium phosphate precipitants such as struvite causing pipe blockages (e.g. Borgerding, 1972; Mohajit et al., 1989; Mamais et al., 1994: Williams, 1999). However, this process has been exploited as a treatment method for removal of the high concentrations of N and/or P commonly found in ADL, particularly in those from digestion of waste sludge from biological phosphorus removal activated sludge systems (Pitman et al., 1989; Pitman, 1999; Battistoni et al., 1997; Woods et al., 1999; Stratful et al., 1999). A model that can conveniently handle three-phase mixed weak acid/base chemistry will be helpful to optimise the aeration treatment method for ADL and to develop and evaluate alternative treatment methods. Further, such a model will find potential application in a variety of other chemical treatment systems.

Model development

The three-phase processes (solid-aqueous-gas) that occur during aeration of ADL are the forward and reverse dissociation processes of the weak acid/base species, precipitation of various magnesium and calcium phosphates and carbonates, and stripping of CO_2 and NH_3. Also, ion pairing effects need to be included because these become significant at TDS > 1 000 mg/ℓ (ionic strength, $\mu > 0.025$) (Loewenthal et al., 1986), and the μ values for the ADL in the batch experiments were measured to be around 0.08 to 0.18 (TDS = 3 200 to 7 200 mg/ℓ, Conductivity 470 to 1 071 mS/m). Also, in a pre-liminary evaluation of the model, model predictions were compared with literature data which included ion pairing.

Aqueous phase mixed weak acid/base chemistry

The aqueous phase weak acid/base chemistry was modelled by including the kinetics for the forward and reverse dissociation reactions of the water, carbonate, phosphate, ammonium and SCFA weak acid/base systems as outlined by Musvoto et al. (1997), with the same kinetic rates and stoichiometry as set out in their Tables 1, 2a, 2b and 2c, compounds 1 to 15 and processes 1 to 6 and 9 to 18. The rates in Table 2c are given as /s. In this paper the basic time unit is /d; the rates have the same numerical value but the units are /d instead of /s.

Ion pairing effects

The most common ion pairs formed in solutions containing calcium and magnesium in the presence of the carbonate, phosphate and ammonia weak acid/base system species are listed in Table 1a together with their stability constants. To include ion pairing in the kinetic model, it was noted that the equilibrium equations for ion pair formation are similar to those representing the dissociation equilibria of weak acid/bases. Accordingly, the ion pairing equilibria were described in terms of the kinetics of the forward and reverse reactions and included in the model in the same manner as outlined by Musvoto et al. (1997) for weak acid/bases. Including the 11 identified ion pair compounds extends the model matrix by 12 compounds from 16 to 27, i.e. magnesium (compound 16) and the 11 ion pair compounds (17 to 27), and the number of processes by 22 from 20 to 41, i.e. one forward and one reverse dissociation process for each ion pair. The ion pair section of the matrix, which is added to the existing model matrix given in Table 1 of Musvoto et al. (1997), is shown in Table 1b. It should be noted that not all the compounds and processes associated with the ion pairs identified for inclusion in the model (Table 1a) are shown in Table 1b, only the first and last two of the 11 ion pairs in Table 1a and one generic ion pair are given for illustrative purposes. Also, some of the columns representing the compounds are duplicated from Table 1 in Musvoto et al. (1997), i.e. columns 5, 8, 11, 12 and 15 for CO_3^{2-}, OH^-, HPO_4^{2-}, PO_4^{3-} and Ca^{2+} respectively, because these compounds also appear in the ion pairing processes. The ion

TABLE 1a
Common ion pairs formed in solutions containing calcium and magnesium with carbonate, phosphate and ammonia weak acid/bases present and their stability constants (pK_{ST}) at 25°C (activity scale). Those from Ferguson and McCarty (1971) in column (a) were included in the model.

No	Ion pair reaction - Ca and Mg	Stability constants pK_{ST} - Sources		
		a	d	e
20	$Ca^{2+} + OH^- \leftrightarrows CaOH^+$	-1.37[b]	-1.15	-1.22
22	$Ca^{2+} + CO_3^{2-} \leftrightarrows CaCO_3(aq)$	-3.2[b]		-3.21
24	$Ca^{2+} + HCO_3^- \leftrightarrows CaHCO_3^+$	-1.26[b]		-2.71
26	$Ca^{2+} + PO_4^{3-} \leftrightarrows CaPO_4^-$	-6.46[c]	-6.5	
28	$Ca^{2+} + H PO_4^{2-} \leftrightarrows CaHPO_4(aq)$	-2.73[c]	-2.7	
30	$Ca^{2+} + H_2PO_4^- \leftrightarrows CaH_2PO_4^+$	-1.41[c]	-1.4	
32	$Mg^{2+} + OH^- \leftrightarrows MgOH^+$	-2.2[b]	-2.56	-2.56
34	$Mg^{2+} + CO_3^{2-} \leftrightarrows MgCO_3(aq)$	-3.4[b]		-2.98
36	$Mg^{2+} + HCO_3^- \leftrightarrows MgHCO_3^+$	-1.16[b]		-4.90
38	$Mg^{2+} + HPO_4^{2-} \leftrightarrows MgHPO_4(aq)$	-2.5[b]	-2.5	
40	$Mg^{2+} + PO_4^{3-} \leftrightarrows MgPO_4^-$	-3.13[b]		

(a) Ferguson and McCarty (1971) from (b) Sillen and Martell (1964) and (c) Chughtai et al. (1968); (d) Stumm and Morgan (1981); (e) Nordstrom et al. (1990).

pairing process rates are defined on the right hand side of Table 1b. The process rate constants were determined in the same manner followed for the weak acid/base dissociation constants (Musvoto et al., 1997), i.e. the rate for the forward ion pair reaction was selected at a very high value (10^7/s, Table 1c) and the rate for the reverse ion pair reaction was then calculated from the appropriate ion pair stability constant (Table 1c); this procedure ensures rapid equilibrium and that the equilibrium species concentrations correspond to those determined by equilibrium chemistry. The ion pair stability constants (pK_{ST}, Table 1c) were regarded as model constants and were not changed in the simulations. The values incorporated in the model are from the literature and are listed in Table 1a; the calculation procedures to adjust these values for Debye-Hückel ionic strength effects using mono-, di- and trivalent activity coefficients (f_i), are given in Table 1c. The ion pair stability constants could not be adjusted for temperature, as no information is available in the literature on this.

TABLE 1b

Matrix representation of the ion pairing reactions of the most common Ca^{2+} and Mg^{2+} ion pairs in solutions containing carbonate and phosphate species. Ion pair stability constants and equilibrium equations are given in Tables 1a and 1c respectively.

Compound number →		5	8	11	12	15	16	17	18	19....	.....	...25	26	27	
Process number ↓		CO_3^{2-}	OH^-	HPO_4^{2-}	PO_4^{3-}	Ca^{2+}	Mg^{2+}	$CaOH^+$	$CaCO_3^0$	A^{X+}	B^{Y-}	AB^{X+Y-}	$MgHPO_4$	$MgPO_4^-$	Process Rate
20	Assoc. of Ca^{2+}, OH^-		-1			-1		+1							$K'_{fca1}[Ca^{2+}][OH^-]$
21	Dissoc. of $CaOH^+$		+1			+1		-1							$K'_{rca1}[CaOH^+]$
22	Assoc. of Ca^{2+}, CO_3^{2-}	-1				-1			+1						$K'_{fca2}[Ca^{2+}][CO_3^{2-}]$
23	Dissoc. of $CaCO_3^0$	+1				+1			-1						$K'_{rca2}[CaCO_3^0]$
.....	Assoc. of A^{X+}, B^{Y-}									-1	-1	+1			$K'_{fST}[A^{X+}][B^{Y-}]$
.....	Dissoc. of AB^{X+Y-}									+1	+1	-1			$K'_{rST}[AB^{X+Y-}]$
38	Assoc. of Mg^{2+}, HPO_4^{2-}			-1			-1						+1		$K'_{fmg4}[Mg^{2+}][HPO_4^{2-}]$
39	Dissoc. of $MgHPO_4^0$			+1			+1						-1		$K'_{rmg4}[MgHPO_4](aq)$
40	Assoc. of Mg^{2+}, PO_4^{3-}				-1		-1							+1	$K'_{fmg5}[Mg^{2+}][PO_4^{3-}]$
41	Dissoc. of $MgPO_4^-$				+1		+1							-1	$K'_{rmg5}[MgPO_4^-]$
	Units	mol/ℓ	mol/ℓ	mol/ℓ	mol/ℓ	mol/ℓ	mol/ℓ	mol/ℓ	mol/ℓ	mol/ℓ	mol/ℓ	mol/ℓ	mol/ℓ	mol/ℓ	

Mineral precipitation

Liquors from anaerobic digesters contain Mg, Ca, free and saline ammonia (FSA), and phosphate and carbonate system species, and under the conditions prevailing when ADL is aerated, the solids most likely to precipitate are various magnesium and calcium carbonates and phosphates, as set out in Table 2. Domains for precipitation of the various forms of these minerals have been delineated in the literature, and are reviewed briefly below to identify the precipitation processes to be included in the model (for a detailed review, see Musvoto et al., 1998).

Magnesium phosphates

From the literature, four possible magnesium phosphate species can crystallise from solutions containing Mg, ammonia and phosphate system species (Table 2): Magnesium ammonium phosphate or struvite ($MgNH_4PO_4 \cdot 6H_2O$), magnesium hydrogen phosphate trihydrate or newberyite ($MgHPO_4 \cdot 3H_2O$) and trimagnesium phosphate in two states of hydration, $Mg_3(PO_4)_2 \cdot 8H_2O$ (bobierrite) and $Mg_3(PO_4)_2 \cdot 22H_2O$. Studies have identified the regions for precipitation of these minerals (e.g. Abbona et al., 1982, 1986, 1988): Struvite precipitates at neutral and higher pH and at Mg/Ca molar ratios > 0.6; newberyite precipitates significantly only at lower pH (< 6.0) and at high concentrations of Mg and P_T; trimagnesium phosphate, which is reported to have a low precipitation rate (Mamais et al., 1994), has never been observed in the pH range expected for aeration of ADL (6 < pH < 9). Accordingly, precipitation of struvite and newberyite were included in the model as processes 42 and 43 respectively (Table 3) using the general kinetic rate formulation of Koutsoukos et al. (1980), see Musvoto et al. (1997) Eq. (6), with the order of reaction n = 3 for struvite (Gunn, 1976) and the default n = 2 for newberyite. This formulation applies only to precipitation and not to dissolution; in the model the equation is valid only if the ionic product is greater than the solubility product - this condition must be checked (Musvoto et al., 1997). ***This restriction applies to all precipitation processes.***

Calcium phosphates

Five calcium phosphate crystalline species can precipitate from solutions containing Ca and P; in order of decreasing solubility these are (Table 2): Hydroxyapatite [HAP, $Ca_5(PO_4)_3OH$],

TABLE 1c
Specific rate constants[3] for ion pair reactions in Tables 1a and 1b. See Loewenthal et al. (1989) for calculation of activity coefficients (f_i) for the different ionic species. The stability constants pK_{ST} values at infinite dilution are given in Table 1a.

No	Process	Specific rate constants					
		Ion pair association reaction		Ion pair dissociation reaction		Stability constant pK_{ST}	
		Symbol	Value	Symbol	Value	Symbol	Value
20..21	$Ca^{2+} + OH^- \leftrightarrows CaOH^+$	K'_{fca1}	$K'_{rca1} \bullet K'_{CaOH+}$	K'_{rca1}	10^7 (/d)	K'_{CaOH+}	$10^{-pKCaOH+} \cdot f_m \cdot f_d / f_m$
22..23	$Ca^{2+} + CO_3^{2-} \leftrightarrows CaCO_3^0$	K'_{fca2}	$K'_{rca2} \bullet K'_{CaCO3}$	K'_{rca2}	10^7 (/d)	K'_{CaCO3}	$10^{-pKCaCO3} \cdot f_d \cdot f_d$
24..37	$A^{X+} + B^{Y-} \leftrightarrows AB^{X+Y-}$	K'_{fST}	$K'_{rST} \bullet K'_{ST}$	K'_{rST}	10^7 (/d)	K'_{ST}	$10^{-pKST} \cdot f_{A(X+)} \cdot f_{B(Y-)} / f_{AB(X+Y-)}$
38..39	$Mg^{2+} + HPO_4^{2-} \leftrightarrows MgHPO_4^0$	K'_{fmg4}	$K'_{rmg4} \bullet K'_{MgHPO4}$	K'_{rmg4}	10^7 (/d)	K'_{MgHPO4}	$10^{-pKMgHPO4} \cdot f_d \cdot f_d$
40..41	$Mg^{2+} + PO_4^{3-} \leftrightarrows MgPO_4^-$	K'_{fmg5}	$K'_{rmg5} \bullet K'_{MgPO4-}$	K'_{rmg5}	10^7 (/d)	K'_{MgPO4-}	$10^{-pKMgPO4-} \cdot f_d \cdot f_t / f_m$

[3]The specific rate constants for ion pairs $CaCO_3^0$, $CaHCO_3^+$ and $CaPO_4^-$ are 1/d, which means in effect these ions pairs do not form. The effect of ion pairing rates on precipitate formation and rates is complex and will be the subject of a subsequent paper.

tri-calcium phosphate (whitlockite) [TCP, $Ca_3(PO_4)_2$], octacalcium phosphate [OCP, $Ca_8(HPO_4)_2(PO_4)_4 \cdot 5H_2O$], monenite (DCP, $CaHPO_4$) and dicalcium phosphate dihydrate (brushite) (DCPD, $CaHPO_4 \cdot 2H_2O$). Thermodynamically HAP is the most stable phase and could be expected to precipitate. However, it has been established that a number of species act as precursors to the precipitation of HAP, such as amorphous calcium phosphate (ACP, with approximate formulation $Ca_3(PO_4)_2 \cdot xH_2O$, similar to TCP, but with no structured crystalline order, Blumenthal et al., 1977; Betts et al., 1981), OCP and DCPD. With time these species may transform to HAP. The precursor species which first precipitate and their transformation are significantly affected by the interaction between pH, Ca and Mg concentrations in the wastewater, as well as the alkalinity and organic material present. From experimental investigations of these processes, it can be concluded that in highly supersaturated solutions containing Ca, Mg and P, DCPD and ACP are the phases that precipitate first, with DCDP precipitating at low pH (<7.0) and ACP at higher pH (Abbona et al., 1986, 1988). Precipitation follows Oswald's rule of stages (when a number of similar solids are highly supersaturated, the least stable solid will precipitate) with the initially formed metastable precursor species ACP and DCPD converting with time to the more thermodynamically stable species of DCP, HAP or TCP. The conversion from the initial to final species takes place via a solution mediated species transition with the initial species dissolving first and the new species growing. Whereas the formation of the first species is a relatively fast process, the growth of the second species is very slow such that the conversion takes a long time (from a minimum of one month to a number of years). The presence of Mg in solution strongly affects the conversion process (Arvin, 1983). Conversion of ACP to the thermodynamically stable species HAP does not take place in solutions with high Mg/Ca molar ratios > 4.0. Other factors such as high pH, high ionic strength, high HCO_3^-/PO_4^{3-} molar ratio, presence of pyrophosphates as well as certain proteins, and lack of HAP seed material also stabilise ACP. Therefore, ACP can be expected to precipitate in wastewaters such as sewage effluents, ADL and sludge dewatering liquors which have characteristics that suppress precipitation of HAP, but promote and stabilise the formation of ACP. Furthermore, in such wastewaters the transformation of ACP to HAP will be retarded so that within the timescale of ADL aeration systems (~60 h), significant HAP is unlikely. For these reasons, ACP was included in the model as the calcium phosphate mineral most likely to precipitate under the conditions present on aeration of ADL, as process 44 (Table 3). The general kinetic rate formulation of Koutsoukos et al. (1980) given by Eq. (6) in Musvoto et al. (1997) was followed for ACP precipitation, with the default order of reaction n = 2.

Calcium carbonates

Three crystalline structure varieties of $CaCO_3$ can precipitate, namely calcite, aragonite and vaterite (Table 2). The species that precipitate have been shown to depend on the temperature, degree of supersaturation, presence of foreign ions as well as the nucleation and crystal growth rates. From the literature, calcite is the thermodynamically stable form at ambient temperature and atmospheric pressure (Roques and Girou, 1974), and will precipitate under the conditions present on aeration of ADL. Accordingly, precipitation of the $CaCO_3$ mineral calcite was retained in the model, i.e. process 19 from Table 1 in Musvoto et al. (1997). The rate of precipitation of $CaCO_3$ is heavily influenced by the presence of Mg, Fe, phosphate system species as well as dissolved organics, which decrease the rate and increase the solubility. These factors were recognised in the determination of the $CaCO_3$ precipitation rate, see Model Validation below.

Other minerals

Other minerals which may precipitate in ADL are magnesium carbonates and calcium magnesium carbonates. Two forms of magnesium carbonates are possible (Table 2), magnesite ($MgCO_3$) and nesquehonite ($MgCO_3 \cdot 3H_2O$). Of the two, $MgCO_3$ is stable below pH ≈10.7 and $MgCO_3 \cdot 3H_2O$ is not; accordingly, $MgCO_3$ precipitation was included in the model as process 45 (see Table 3), using the Koutsoukos et al. (1980) kinetic rate formulation given by Eq. (6) in Musvoto et al. (1997), with the default order of reaction

ISSN 0378-4738 = Water SA Vol. 26 No. 4 October 2000

TABLE 2
Minerals that could possibly precipitate on aeration of ADL; values of solubility products at 25°C and infinite dilution obtained from databases in the literature. The five compounds marked with an * were included in the kinetic model.

Solubility equilibria		pK_{SP} at 25°C			
Mineral	**Reaction**	**Stumm and Morgan (1981)**	**Nordstrom et al. (1990)**	**JESS (Murray and May, 1996)**	**Other sources**
*Calcite/Aragonite/Vaterite	$CaCO_3 \leftrightarrows Ca^{2+} + CO_3^{2-}$	8.42; 8.22	8.48; 8.34	8.5; 8.22	8.3[e] ; 7.8[f] ; 6.7[h]
*Magnesite	$MgCO_3 \leftrightarrows Mg^{2+} + CO_3^{2-}$	7.46; 8.2		7.46; 8.2	5.9[e] ; 7.9[f]
Nesquehonite	$MgCO_3.3H_2O \leftrightarrows Mg^{2+} + CO_3^{2-} + 3H_2O$	5.19		4.67; 5.19	
Dolomite (disordered)	$CaMg(CO_3)_2 \leftrightarrows Ca^{2+} + Mg^{2+} + 2CO_3^{2-}$	16.7	16.54	16.5	
Dolomite (ordered)	$CaMg(CO_3)_2 \leftrightarrows Ca^{2+} + Mg^{2+} + 2CO_3^{2-}$		17.09	16.98	17[f]
Huntite	$CaMg(CO_3)_4 \leftrightarrows Ca^{2+} + Mg^{2+} + 4CO_3^{2-}$				N/A
Calcium hydroxide	$Ca(OH)_2(s) \leftrightarrows Ca^{2+} + 2OH^-$	5.2	5.2		
Brucite	$Mg(OH)_2(s) \leftrightarrows Mg^{2+} + 2OH^-$	11.16	11.16		10.7[e]
HAP	$Ca_{10}(PO_4)_6(OH)_2(s) \leftrightarrows 10Ca^{2+} + 6PO_4^{3-} + 2OH^-$	114		57.5; 48.6	57.8[f]
TCP	$Ca_3(PO_4)_2 \leftrightarrows 3Ca^{2+} + 2PO_4^{3-}$			32.63; 32.7	
OCP	$Ca_8(HPO_4)_2(PO_4)_4.5H_2O \leftrightarrows 8Ca^{2+} + 2HPO_4^{2-} + 4PO_4^{3-} + 5H_2O$				94.16[i]; 72.53[i]
DCP	$CaHPO_4(s) \leftrightarrows Ca^{2+} + HPO_4^{2-}$	6.6		6.6; 6.5	
DCPD	$CaHPO_4.2H_2O \leftrightarrows Ca^{2+} + HPO_4^{2-} + 2H_2O$	6.6		6.6	
*ACP	$Ca_3(PO_4)_2.xH_2O \leftrightarrows 3Ca^{2+} + 2PO_4^{3-} + xH_2O$	31.45			26.0[a]; 25.2[b], 24[e];25.46[g]
*Struvite	$MgNH_4PO_4.6H_2O(s) \leftrightarrows Mg^{2+} + NH_4^+ + PO_4^{3-} + 6H_2O$	12.6		13.16	12.6[a]; 12.72[c]; 13.15[d], 13[e]
*Newberyite	$MgHPO_4.3H_2O(s) \leftrightarrows Mg^{2+} + HPO_4^{2-} + 3H_2O$			5.8	5.51[c] ; 5.8[d]
Bobierrite	$Mg_3(PO_4)_2.8H_2O(s) \leftrightarrows 3Mg^{2+} + 2PO_4^{3-} + 8H_2O$			25.2	25.2[d]
Trimagnesium phosphate	$Mg_3(PO_4)_2.22H_2O(s) \leftrightarrows 3Mg^{2+} + 2PO_4^{3-} + 22H_2O$				23.1[d]

Notes: 1. Temperature dependency of solubility products for some of the reactions has been given by Stumm and Morgan (1981) and Nordstrom et al. (1990).
2. Lettered references apply to the following: [a] Butler (1964); [b] Meyer and Eanes (1978) cited by Moutin et al. (1992); [c] Abbona et al. (1982); [d] Taylor et al. (1963) cited by Scott et al. (1991); [e] Mamais et al. (1994); [f] Ferguson and McCarty (1971). [g] Hoffmann and Marais (1977) - value from Butler (1964) corrected for ionic strength; [h] Wiechers et al. (1980); [i] Verbeeck and Devenyns (1992).

TABLE 3

Matrix representation of the processes of precipitation and gas stripping included in the three-phase mixed weak acid/base kinetic model. The single phase aqueous forward and reverse dissociation processes of weak acid/base species and the three-phase processes of the carbonate system are given in Table 1 of Musvoto et al. (1997) with the same numbering of the compounds.

No	Compound →	1	2	3	4	5	7	8	9	10	11	12	13	14	15	16	Rate
	Process ↓	NH_4^+	NH_3	$H_2CO_3^*$	HCO_3^-	CO_3^{2-}	H^+	OH^-	H_3PO_4	$H_2PO_4^-$	HPO_4^-	PO_4^{3-}	HA	A^-	Ca^{2+}	Mg^{2+}	
42	Precipitation of $MgNH_4PO_4$	-1										-1				-1	$K'_{pptStruv}([Mg^{2+}]^{1/3}[NH_4^+]^{1/3}[PO_4^{3-}]^{1/3} - K'_{SPStruv}{}^{1/3})^3$
43	Precipitation of $MgHPO_4$										-1					-1	$K'_{pptNewb}([Mg^{2+}]^{1/2}[HPO_4^{2-}]^{1/2} - K'_{SPNewb}{}^{1/2})^2$
44	Precipitation of $Ca_3(PO_4)_2$											-2/3			-1		$K'_{pptACP}([Ca^{2+}]^{3/5}[PO_4^{3-}]^{2/5} - K'_{SPACP}{}^{1/5})^2$
45	Precipitation of $MgCO_3$					-1										-1	$K'_{pptMgCO3}([Mg^{2+}]^{1/2}[CO_3^{2-}]^{1/2} - K'_{SPMgCO3}{}^{1/2})^2$
46	Stripping of NH_3		-1														$K'_{rNH3}[NH_3]$
	Units	mol/ℓ	mol/ℓ	mol/ℓ	mol/ℓ	mol/ℓ	mol/ℓ	mol/ℓ	mol/ℓ	mol/ℓ	mol/ℓ	mol/ℓ	mol/ℓ	mol/ℓ	mol/ℓ	mol/ℓ	

n = 2. Two mixed carbonates of Ca and Mg occur in nature, dolomite [$CaMg(CO_3)_2$] and huntite [$CaMg(CO_3)_4$] (Table 2). However, the conditions under which these precipitate are not well understood, and attempts to precipitate dolomite under atmospheric conditions have not been successful (Mamais et al., 1994). Accordingly these minerals were not considered for inclusion in the model. Also not included in the model are $Ca(OH)_2$ and $Mg(OH)_2$ (Brucite) (Table 2). These minerals precipitate at high pH (>10), so that at the relatively low pH of the batch tests (<9.5) and in the presence of the other precipitating minerals incorporating Ca and Mg discussed above, the ionic products of the hydroxide and Ca and Mg species at pH < 9.5 would not exceed the solubility products of $Mg(OH)_2$ and $Ca(OH)_2$.

Solubility products

Solubility products in the literature for the five minerals identified above as likely to precipitate on ADL aeration (calcite, struvite, newberyite, ACP and magnesite) are listed in Table 2. These solubility products are at 25°C and infinite dilution, i.e. for ideal solutions unless otherwise indicated. To account for the effect of ionic strength in non-ideal solutions, the solubility products were adjusted following the Debye-Hückel theory for low and medium salinity waters (Loewenthal et al., 1989; Musvoto et al., 1998). The solubility products could not be adjusted for temperature, since no information in the literature is available on this. The solubility products were regarded as model constants in that once the appropriate values were selected from the literature, they were not changed except for the ionic strength adjustments above. The values at 25°C and infinite dilution included in the model for the five minerals are given in Table 7. Throughout the paper, the term model constants applies to those constants that were not changed in the model; the term calibration constants are the constants that were changed to fit the model predicted results to the experimental data.

Gas stripping

Gases expected to be stripped from ADL are CO_2 and NH_3. The exchange of CO_2 between the liquid and gas phases has already been included in the model as processes 7 and 8 (see Tables 1, 2b and 2c of Musvoto et al., 1997). A similar approach was followed for NH_3, except that for NH_3 it was assumed that the atmosphere acts as an infinite sink; thus the dissolution of NH_3 from the atmosphere into solution was not included in the model, only NH_3 expulsion as given by process 46 in Table 3. In the rate expressions for CO_2 and NH_3 stripping and CO_2 dissolution, the rate constants (K'_{rCO2}, K'_{rNH3} and K'_{fCO2}, respectively) need to be determined because these values are influenced by a number of factors, such as turbulence, mixing, diffusivity and temperature. These rates therefore need to be calibrated for the specific situation being modelled, in this case the aeration batch test conditions. Musvoto et al. (1997) showed that the gas stripping rate is equal to the overall liquid phase mass transfer rate coefficient K'_{La}, viz. $K'_{rCO2} = K'_{La,CO2}$ and $K'_{rNH3} = K'_{La,NH3}$ and that the dissolution rate of CO_2 (K'_{fCO2}) is related to its stripping rate (K'_{rCO2}) through Henry's law constant ($K'_{H,CO2}$), viz. $K'_{fCO2} = K'_{H,CO2} \cdot RT \cdot K'_{rCO2}$. Hence, once the K'_H is known (model constant) for the gas being stripped or dissolved, the only unknown (calibration constant) is the K'_{La} coefficient. Note that for consistency in this discussion, as also in Musvoto et al. (1997), K'_H and K'_{La} (dashed) are used indicating that the associated gas concentrations are defined in molar [ ], not activity ( ), terms. However, because the gases considered are non-ionic, activity and molar concentrations are equal, hence $K'_H = K_H$ and $K'_{La} = K_{La}$.

Munz and Roberts (1989) review the fundamental concepts of

mass transfer across the gas-water interface. They concluded that provided the dimensionless Henry's law constant $\{H_c = 1/(K_H \cdot RT)\}$ for the gas is greater than 0.55, then oxygen can be used as a reference compound and the K_{La} value will be proportional to K_{La} of oxygen (for details see Musvoto et al., 1998). For CO_2, $H_c = 0.95$ at 20°C but for NH_3, $H_c = 0.011$ at 20°C (Katehis et al., 1998). Therefore in the model, the K_{La} values for oxygen and CO_2 are proportional and only the former needs to be calibrated. Because $H_c < 0.55$ for NH_3, $K'_{La,NH3}$ is not proportional to the reference gas oxygen $K'_{La,O2}$ and the $K'_{La,NH3}$ has to be calibrated independently. In the aeration batch tests, the dissolved oxygen (DO) concentration was not measured and the DO was not included in the model as a compound. Therefore, even though $K'_{La,CO2}$ is defined in terms of $K'_{La,O2}$, in effect only $K'_{La,CO2}$ was determined by calibration against measured data. The general approach to modelling CO_2 gas exchange via the reference gas oxygen was adopted so that if, in further extensions of the model, other gases are included with $H_c > 0.55$, their K'_{La} rates would be proportional to that of oxygen. The K'_{La} rates for CO_2 and NH_3 are calibration constants in the model.

Preliminary model validation

A preliminary calibration and validation of the model for the chemical processes of precipitation was carried out by comparing predictions with information available in the literature. Two literature information sets were used, both restricted to initial and final state equilibrium conditions: the equilibrium based model of Loewenthal et al. (1994) for the precipitation of the single mineral struvite; and the experiments of Ferguson and McCarty (1971) for the precipitation of several Ca and Mg minerals from solutions containing phosphate and carbonate system species. All kinetic model simulations were done with the computer programme Aquasim (Reichert, 1994).

Loewenthal et al. (1994) equilibrium model for struvite precipitation

Loewenthal et al. (1994) developed an equilibrium chemistry based model for struvite precipitation which was subsequently coded into a computer programme called Struvite 3.1 by Loewenthal and Morrison (1997). Equilibrium conditions predicted by this programme, for the two solutions discussed by Loewenthal et al. (1994) were compared with the predictions of the kinetic model developed above, including processes 1 to 6, 9 to 14 and 17 to 18 for the aqueous species of the ammonia, carbonate, phosphate and water weak acid/base systems (Table 1 in Musvoto et al., 1997) and process 42 for struvite precipitation (Table 3). Ion-pairing effects (processes 20 to 41, Table 1a) were not included because the model of Loewenthal et al. (1994) does not consider these. The TDS concentrations of the two solutions, which are required as input to Struvite 3.1, were calculated from the ionic strength of the ammonium chloride, magnesium chloride and potassium phosphate species making up the solutions and the TDS - ionic strength (μ) relationship given by Loewenthal et al. (1989), i.e. $\mu = 2.5 \cdot 10^{-5}$ (TDS-20); viz., μ=0.0826 giving a TDS of 3 325 mg/ℓ for Solution 1 and μ = 0.0706 giving a TDS of 2 844 mg/ℓ for Solution 2 (see Table 4a). The initial total species concentrations of the phosphate (P_T), short chain fatty acid (A_T) and ammonia (N_T) systems, the magnesium concentration (Mg), the partial pressure of CO_2 (which fixes the total species concentration of the carbonate system, C_T) and pH for the two solutions are listed in Table 4a. The weak acid/base pK values and their temperature sensitivities, and the solubility product for struvite (no temperature correction) included in Struvite 3.1 are those given by Loewenthal et al. (1994) (see also Loewenthal et al., 1989 or Musvoto et al., 1997 Table 2c). These were included also in the kinetic model as model constants (not changed). The initial total alkalinities (T Alk) were calculated by the Struvite 3.1 equilibrium model as 1 284 and 990 mg/ℓ as $CaCO_3$ for Solutions 1 and 2 respectively, and are with respect to the most protonated species of each of the weak acid/base systems, viz. the H_2CO_3*/H_3PO_4/NH_4^+/HAc alkalinity. The initial H_2CO_3*/H_3PO_4/NH_4^+/HAc alkalinity (T Alk) calculated by the kinetic model was 1275 mg/ℓ as $CaCO_3$ (0.0255 mol/ℓ) for Solution 1 and 981 mg/ℓ as $CaCO_3$ (0.0196 mol/ℓ) for Solution 2. Thus, Struvite 3.1 and the kinetic model give virtually identical initial H_2CO_3*/H_3PO_4/NH_4^+/HAc (total) alkalinity values for both solutions. This indicated that the initial conditions specified in both models were virtually identical.

It should be noted that the modified Gran titration method for determining the total alkalinity of a mixed weak acid/base system developed by Loewenthal et al. (1989) uses $H_2PO_4^-$ as reference species for the phosphate system, viz. the H_2CO_3*/$H_2PO_4^-$/NH_4^+/HAc alkalinity. Therefore, if the modified Gran titration method of Loewenthal et al. (1989) is used to determine the H_2CO_3*/$H_2PO_4^-$/NH_4^+/HAc alkalinity of a mixed weak acid/base solution, this alkalinity needs to be recalculated in terms of the H_3PO_4 reference species for the phosphate system before insertion into the Struvite 3.1 model. This conversion is simple, because from Loewenthal et al. (1989), H_2CO_3*/H_3PO_4/NH_4^+/HAc alkalinity = H_2CO_3*/$H_2PO_4^-$/NH_4^+/HAc alkalinity + P_T, all in mol/ℓ; if the alkalinities are in mg/ℓ as $CaCO_3$ and P_T in mgP/ℓ (as in Struvite 3.1), then $50/31 \cdot P_T$ is added to the H_2CO_3*/$H_2PO_4^-$/NH_4^+/HAc alkalinity to give the H_2CO_3*/H_3PO_4/NH_4^+/HAc alkalinity, e.g. for Solution 1 the H_2CO_3*/$H_2PO_4^-$/NH_4^+/HAc alkalinity would be $1284 - 400 \cdot 50/31 = 645$ mg/ℓ as $CaCO_3$ and for Solution 2, the H_2CO_3*/$H_2PO_4^-$/NH_4^+/HAc alkalinity would be $990 - 300 \cdot 50/31 = 506$ mg/ℓ as $CaCO_3$.

In Struvite 3.1, the ionic strength (μ), the mono-, di- and tri-valent ion activity coefficients (f_m, f_d, f_t), and hence the pK' values for non-ideal solutions, are determined from the input TDS, and the first iteration to calculate the equilibrium condition is based on this initial μ. A revised μ is then calculated taking into account the change in ionic species due to precipitation of struvite. A revised equilibrium condition is then determined from the revised μ and this equilibrium condition is accepted as the final condition. In the kinetic model the ionic strength, mono-, di- and tri-valent ion activity coefficients (f_m, f_d, f_t), and hence the pK' values for non-ideal solutions, are embedded within the equations for the kinetic constants of the model and therefore any change in ionic strength due to precipitation is taken into account at each integration step in an integrated and seamless way.

The initial and final equilibrium conditions predicted by Struvite 3.1 and the kinetic model for the two solutions are listed in Table 4a. It can be seen for Solution 1, which does not contain carbonate system species, the kinetic model predicts lower dissolved species concentrations (by about 0.0006 mol/ℓ) and a lower pH by 0.19 units. Also the concentration of struvite precipitated is almost 20% more in the kinetic model. The difference in the species concentrations and struvite precipitated between that predicted by the kinetic model and by Struvite 3.1 is smaller for Solution 2, viz. 0.0002 mol/ℓ lower and 7% more struvite precipitated with the kinetic model. However, the pH difference is greater, viz. 0.23 pH units lower in the kinetic model. In seeking the reason for these differences, ionic speciation at the final conditions predicted by the two models was undertaken. It was found that for both solutions the struvite ionic product calculated from the final condition predicted

TABLE 4a

Initial and final concentrations for the two struvite precipitation solutions given by Loewenthal et al. (1994) comparing the kinetic model predictions with the Struvite 3.1 equilibrium struvite precipitation model of Loewenthal and Morrison (1997). Ion pairing not included in both models.

Parameter	Solution 1 (T=20°C, [1]TDS=3325 mg/ℓ)						Solution 2 (T=20°C, [1]TDS=2844 mg/ℓ)					
	Initial conditions		Final Struvite 3.1		Final kinetic model		Initial Conditions		Final Struvite 3.1		Final kinetic model	
	mg/ℓ	mol/ℓ	mg/ℓ	mol/ℓ	mg/ℓ	mol/ℓ	mg/ℓ	mol/ℓ	mg/ℓ	mol/ℓ	mg/ℓ	mol/ℓ
[2]T Alk	1284	0.0257	734	0.0147	620	0.0124	990	0.0198	554	0.0111	507	0.0102
N_T	300	0.0214	249	0.0178	238	0.0170	250	0.0179	209	0.0149	207	0.0148
P_T	400	0.0129	286	0.0092	264	0.0085	300	0.0097	210	0.0068	203	0.0066
Mg	200	0.0083	111	0.0046	96	0.0040	200	0.0083	129	0.0054	125	0.0052
pH	8.04		7.04		6.85		7.96		7.11		6.88	
pCO_2	0		0		0		0.00037		0.00037		0.00037	
Struvite precipitated (mg/ℓ)			503		601		-		399		426	

1. Total dissolved solids (TDS) concentration was calculated from the ionic strength of the ammonium chloride, magnesium chloride and potassium phosphate species making up the solution and the TDS - m relationship given by Loewenthal et al. (1989), i.e. $\mu = 2.5x10^{-5}$(TDS-20); for Solution 1, $\mu = 0.0826$ and for Solution 2 $\mu = 0.0706$.
2. Total alkalinity (T Alk) with respect to the H_2CO_3*/H_3PO_4/NH_4^+/HAc reference species as given by Struvite 3.1. In these two solutions the total HAc concentration (A_T) was zero.

TABLE 4b

Speciation results of the Struvite 3.1 struvite precipitation equilibrium model final condition (Table 4a) and the kinetic model (KinM) results using this final condition as initial condition.

Parameter	Solution 1				Solution 2			
	Struvite 3.1 final condition as KinM initial condition		Kinetic Model final condition		Struvite 3.1 final condition as KinM initial condition		Kinetic Model final condition	
	mg/ℓ	mmol/ℓ	mg/ℓ	mmol/ℓ	mg/ℓ	mmol/ℓ	mg/ℓ	mmol/ℓ
T Alk	734	0.0147	706	0.0141	554	0.0111	476	0.0095
N_T	249	0.0178	242	0.0173	209	0.0149	203	0.0145
P_T	285	0.0092	270	0.0087	210	0.0068	198	0.0064
Mg	110	0.0046	86	0.0041	129	0.0054	119	0.0050
pH	7.04		6.86		7.11		6.90	
Ionic product	$8.7•10^{-12}$		$4.8•10^{-12}$		$8.4•10^{-12}$		$4.5•10^{-12}$	
Solublity product	$5.1•10^{-12}$		$4.8•10^{-12}$		$4.6•10^{-12}$		$4.5•10^{-12}$	
pCO_2	0		0		0.00037		0.00037	
Struvite precipitated	0		68		0		58	

by Struvite 3.1 was somewhat greater than the solubility product (see Table 4b). This indicated that the Struvite 3.1 predicted final condition was not at equilibrium. For the kinetic model the struvite ionic product calculated from the final condition was equal to the solubility product for both solutions indicating that an equilibrium condition had been correctly reached. To check whether or not the Struvite 3.1 predicted final condition was at equilibrium, this final condition for the two solutions was given as initial conditions to the kinetic model, taking due account of the ionic strength. The results predicted by the kinetic model, including the struvite ionic and solubility products, are given in Table 4b. For both solutions, precipitation is predicted to continue with a further 68 and 58 mg/ℓ struvite predicted to precipitate from Solution 1 and 2 respectively to reach equilibrium. The pH of this revised equilibrium

condition is only 0.02 pH units from that predicted by the kinetic model from the initial conditions (Table 4a) and the ionic product is equal to the solubility product (Table 4b).

From the comparison of the Struvite 3.1 equilibrium model and the kinetic model, it can be concluded that the kinetic model identifies the equilibrium condition for a single precipitate accurately and precisely, and that the differences between this condition and the equilibrium condition predicted by Struvite 3.1 lie in the handling of ionic strength and in the algorithm for estimating the equilibrium pH in Struvite 3.1. The advantage of the Struvite 3.1 programme is that it is very simple to use and gives an answer very quickly (< 1 s), which although not exact, is attractive to practising engineers and scientists in the wastewater treatment field. In contrast, the kinetic model is more accurate but requires significant lead-in time to master confidently, particularly if the three-phase mixed weak acid/base kinetic model as described in this paper has to be coded from scratch into a computer programme such as Aquasim (Reichert, 1994).

Experiments of Ferguson and McCarty (1971)

Ferguson and McCarty (1971) report data on precipitation of Ca and Mg minerals from solutions containing carbonate and phosphate system species, and the kinetic model predictions were compared with this data. The data of Ferguson and McCarty includes ion-pairing so this was included in the kinetic model (processes 20 to 41, Table 1b). Struvite precipitation (process 42 in Table 3) was not included because the solutions did not contain NH_4^+ species. Precipitation of Newberyite ($MgHPO_4$) (process 43 in Table 3) was also not included because it precipitates significantly only at low pH (<7), significantly lower than the pH range of the Ferguson and McCarty experiments, pH>8 - in the ADL aeration batch tests described below (7 < pH < 9.5), $MgHPO_4$ precipitation was included and it formed less than 0.3% of the precipitate formed. Ferguson and McCarty accepted that the calcium phosphate mineral formed in their experiments was hydroxyapatite (HAP, $Ca_{10}(PO_4)_6(OH)_2$, see Table 2). However, in the discussion above on calcium phosphate mineral precipitation, it is concluded that amorphous calcium phosphate (ACP, $Ca_3(PO_4)_2 \cdot xH_2O$) would be a more likely precipitant. Also, x-ray diffraction by Ferguson and McCarty indicate the presence of tricalcium phosphate, which has the same formula as ACP. Therefore the precipitation of ACP (process 44 in Table 3) rather than HAP was included in the model. Calcite ($CaCO_3$) and magnesite ($MgCO_3$) also can be expected to precipitate in the Ferguson and McCarty experiments (process 19, Musvoto et al., 1997, Table1 and process 45 Table 3 respectively). Thus, processes included in the model were 1 to 6, 9 to 15 and 17 to 18 (Musvoto et al., 1997 - Table 1) for the forward and reverse weak acid/base dissociations, processes 20 to 41 (Table 1b) for ion-pairing, and 19 (Musvoto et al., 1997 - Table 1) and 44 and 45 (Table 3) for the precipitation of Calcite ($CaCO_3$), ACP and Magnesite ($MgCO_3$) respectively.

Experiments 4 (Exp. 4) and 5 (Exp. 5) were selected from Ferguson and McCarty for simulation, because these two appeared the most suitable for multi precipitate formation modelling and the most internally consistent of the six experiments reported. These experiments were conducted at 29°C. The pK values and their temperature sensitivities for the water, carbonate, phosphate, ammonia and short chain fatty acid weak acid/base systems were included in the model as model constants (not changed); values were those given by Loewenthal et al. (1989) (see also Loewenthal et al., 1994 or Musvoto et al., 1997) which are the same as those used in the comparison with the Struvite 3.1 model described above. The stability constants for the 11 ion pairs (not adjusted for temperature) are those from Ferguson and McCarty and are given in Table 1a under column a. These were also included in the model as model constants (not changed).

The initial ionic strength (μ) was calculated from the ionic species making up the solutions and for Exps. 4 and 5 this was 0.057 and 0.067 respectively. The solubility product values given as input to the model for the three minerals that were identified to precipitate were obtained from Ferguson and McCarty ($CaCO_3$ and $MgCO_3$) and Hoffmann and Marais (1977) (ACP) and are given in Table 5, i.e. for Exp. 4 (pH < 9) $CaCO_3$ 6.8, $MgCO_3$ 6.7 and ACP 25.46 and for Exp. 5 (pH > 9) $CaCO_3$ 6.5, $MgCO_3$ 6.6 and ACP 25.46. These values were not adjusted for temperature. The values for the first two minerals are the activity product (pA) values (which include adjustment for ionic strength) at equilibrium measured by Ferguson and McCarty. The activity product values are equivalent to the thermodynamic solubility product (Ferguson and McCarty, 1971) and accordingly were given as input to the model as such; in the model these are appropriately adjusted for ionic strength to give the apparent solubility products which are in terms of the molar concentrations used in the model. The measured activity product values were considered more suitable for simulating the experiments than the 7.8 and 7.9 solubility product values at infinite dilution quoted for pure solutions of $CaCO_3$ and $MgCO_3$ respectively by Ferguson and McCarty (1971) (see Table 2), because the solubility products for $CaCO_3$ and $MgCO_3$ are influenced by the presence of Mg and Ca respectively, and the activity products were measured for the experiments being simulated and take these effects into account. The value for ACP is the activity product value from Hoffmann and Marais (1977) (see Table 2). During the simulation, the ionic strength was continually calculated to take due consideration of changes in ionic concentrations as a result of mineral precipitation. Hence, the dissociation, stability and solubility constants/products were continually adjusted for ionic strength as the simulation proceeded to equilibrium. In order to keep the pH constant at the initial values as reported by Ferguson and McCarty, OH^- or H^+ dosing was included in the simulations.

With regard to precipitation rate constants, Ferguson and McCarty did not report time dependent data, only the initial and final (equilibrium) concentrations. Thus, only the final steady state (equilibrium) results of the model could be evaluated, not the mineral precipitation rates. However, in the experiments of Ferguson and McCarty minerals precipitate which compete for the same species, e.g. ACP and $CaCO_3$ both include Ca. In situations where competing minerals precipitate, it is possible that the final equilibrium condition will be influenced by the relative rates of precipitation of the competing minerals. Thus, in simulating the data of Ferguson and McCarty, although only the initial and final equilibrium states are given, the rates of precipitation were varied to evaluate the effect on the predicted final equilibrium state. From these simulations it was found that for the selected experiments the final equilibrium state was relatively independent of the precipitation rate constants, provided the precipitation rate constant for ACP was much larger than those for $CaCO_3$ and $MgCO_3$. Accordingly, the precipitation rates used for the simulations of both experiments were ACP 350/d, $CaCO_3$ 0.05/d and $MgCO_3$ 0.05/d. These rates were determined by visually fitting simulated to experimental data.

The measured and predicted final species concentrations remaining in solution for Exps. 4 and 5 are given in Table 5. Also given in Table 5 for both experiments are the concentrations of Ca, Mg, P_T and C_T precipitated, as calculated from the difference between the kinetic model predicted initial and final concentrations, and as given by Ferguson and McCarty from measurements

Table 5
Initial and final concentrations for two Ferguson and McCarty (1971) mineral precipitation experiments (4 and 5) comparing the kinetic model predictions with experimental observation. With ion pairing. Temperature = 29°C.

Parameter	Experiment 4			Experiment 5		
	Initial conditions	Final Ferg & McC	Final kinetic model	Initial conditions	Final Ferg & McC	Final kinetic model
	mmol/ℓ	mmol/ℓ	mmol/ℓ	mmol/ℓ	mmol/ℓ	mmol/ℓ
μ	0.057	-	0.043	0.067	-	0.053
Ca_T	5.0	1.85	1.39	5.0	0.5	0.65
Mg_T	2.0	1.65	1.72	2.0	1.2	0.68
P_T	2.0	0.33	0.16	2.0	0.13	0.33
C_T	30.0	25.0	28.88	30.0	29.0	26.8
Na_T	40.0	-	-	59.5	-	-
Cl_T	14.0	-	-	14.0	-	-
pH	8.11	8.11±0.2*[1]	8.11	10.06	10.06±0.2*[1]	10.06
Concentrations precipitated (mmolℓ)						
Ca	-	3.52	3.61	-	4.55	4.35
Mg	-	0.29	0.28	-	0.88	1.32
P	-	2.57	1.84	-	2.95	1.67
C_T	-	1.35	1.12	-	2.74	3.16
Minerals precipitated as predicted by kinetic model (mmol/ℓ)						
ACP	-	-	0.92	-	-	0.84
$CaCO_3$	-	-	0.84	-	-	1.84
$MgCO_3$	-	-	0.28		-	1.32
Solubility product values (pK_{SP})						
ACP	-	-	25.46*[2]	-	-	25.46*[2]
$CaCO_3$	-	6.8*[3]	6.8*[3]	-	6.5*[3]	6.5*[3]
$MgCO_3$	-	6.7*[3]	6.7*[3]	-	6.6*[3]	6.6*[3]

*[1] Ferguson and McCarty (1971) state that the final pH was within 0.2 pH units of initial pH.
*[2] From Hoffmann and Marais (1977) - see Table 2.
*[3] Activity product values (which include correction for ionic strength) measured by Ferguson and McCarty (1971). The kinetic model results are based on these pK_{SP} values.

with x-ray diffraction. In comparing the kinetic model predicted results with those measured by Ferguson and McCarty, a difficulty is the lack of consistency in the measured data. For the kinetic model predictions, the concentration of Ca, Mg, P_T and C_T precipitated can be reconciled with the precipitated minerals (since these are calculated from the difference between initial and final soluble concentrations). However, in the measured results the concentrations of species precipitated are not equal to the difference between the initial and final soluble concentrations, e.g. in both experiments the measured precipitated P_T concentrations (2.57 and 2.95 mmol/ℓ respectively) are both greater than the difference between the measured initial and final P_T concentrations (1.67 and 1.87 mgP/ℓ respectively). The inconsistencies in the experimental results make a very close correlation between predicted and experimental results unrealistic. Taking the above into account, from Table 5 the predicted and measured final concentrations and concentrations of species precipitated match reasonably closely. Also, the kinetic model predicts correctly the expected precipitation behaviour; from Table 5, in both experiments 4 and 5 about 0.93 mmol/ℓ ACP was formed and, as expected, a significantly larger $CaCO_3$ and $MgCO_3$ concentration precipitated at high pH (Exp. 5) than at low pH (Exp. 4). Taken overall it appeared that the kinetic model performed well with multiple mineral precipitation and therefore was deemed sufficiently robust and stable to model the unsteady state behaviour of multiple mineral precipitation in aeration treatment of ADL.

Experimental investigation

Having completed a preliminary validation of the model for single and multiple mineral precipitation with information in the literature, the model was applied to describe the time dependent three-phase weak acid/base reactions that occur when ADL is aerated. No suitable data in the literature were available on this, so an experimental investigation was undertaken to gather the appropriate data. Aeration of ADL from a spent wine UASB digester (UASBDL) and an anaerobic digester treating sewage sludge (SSADL) was investigated.

Experimental procedure for UASBDL

Liquor from a UASB digester treating grape wine distillery waste at Stellenbosch Farmers' Winery (Wellington, South Africa) was collected directly into sealed pressurised containers. Care was taken that CO_2 loss was minimised during collection, to limit precipitation of minerals before the start of experiments. The containers were stored in the laboratory at 20°C. Five litre samples of the liquor were placed in a batch reactor, again taking care to minimise CO_2 loss, and the liquor was aerated for at least 24 h. At frequent intervals, 100 mℓ and 10 mℓ samples were drawn from the batch reactor for analysis. The pH in the reactor was recorded regularly throughout the experiment and the temperature controlled to 20°C.

Immediately after sampling, the 10 mℓ sample was directly analysed for FSA without prior filtration. Experience had shown that significant loss of ammonia occurred during filtration at high pH. The 100 mℓ sample was immediately vacuum filtered through 0.45μm filters and the filtrate was divided into two. To one filtrate

sample, a few drops (≈1.5 mℓ) of concentrated nitric acid (HNO_3) were added to reduce the pH to below 2 and so prevent further precipitation. The acidified filtered sample was analysed for the following:

- Ca, Mg and Fe: By emission spectroscopy using the inductively coupled plasma (ICP) method (*Standards Methods*, 1985). The Fe concentration was found to be very low (<1 mg/ℓ) and its analysis was thus discontinued after the first few batch tests. In hindsight this was an error because it was later learned that the $CaCO_3$ precipitation rate is very sensitive to even low concentrations of Fe.
- Phosphate system species (P_T): Molybdate/vanadate colour reaction and/or ICP method (*Standard Methods*, 1985).

The second filtered sample was not acidified and was analysed for:

- Carbonate system species (C_T): This parameter was calculated after directly measuring the $H_2CO_3^*$ alkalinity and pH with the 5-point pH titration method of Moosbrugger et al. (1992), which is based on the mixed weak acid/base characterisation method of Loewenthal et al. (1989) and takes due account of the presence of ammonia (N_T), phosphate (P_T) and short-chain fatty acid (A_T) weak acid/base system species. [*Loss of CO_2 during vacuum filtration does not significantly affect the H_2CO_3* alkalinity. Determination of the H_2CO_3* alkalinity requires knowing the carbonic acid (H_2CO_3*) equivalence point pH. While by definition the H_2CO_3* alkalinity is independent of CO_2 loss or gain, loss or gain of CO_2 does influence the H_2CO_3* equivalence point pH, which increases slightly with loss of CO_2 (or C_T decrease). However, the difference in H_2CO_3* equivalence point pH does not significantly affect the H_2CO_3* alkalinity because the H_2CO_3* equivalence point is in an area of low buffer capacity for the carbonate system. Moreover, the mixed weak acid/base characterisation method of Loewenthal et al. (1989) does not require the H_2CO_3* equivalence point pH to be known to determine the H_2CO_3* alkalinity. The 5 pH point titration method of Moosbrugger et al. (1992) was developed not so much to obviate the use of expensive instrumentation for analysing inorganic carbon (C_T) and short chain fatty acids (A_T), but to have a measurement method for C_T that is insensitive to CO_2 loss.]*
- Short chain fatty acids (SCFA, A_T): 5-point pH titration method of Moosbrugger et al. (1992).

Experimental procedure for SSADL

Anaerobically digested sludge liquor was obtained from the anaerobic digesters at Cape Flats Wastewater Treatment Plant (WWTP) (Cape Town, South Africa). These digesters (with retention time of 10 to 12 d) treat a blend of primary and secondary waste activated sludge (WAS) from a 5 stage modified Bardenpho biological nutrient (nitrogen and phosphorus) removal activated sludge system, treating 150 Mℓ/d of wastewater, primarily of domestic origin. Although originally designed for biological excess P removal (BEPR), little BEPR took place at the time of testing with the result that the ADL did not contain the elevated P and Mg concentrations characteristic of ADL from BEPR plants. The anaerobically digested sludge was collected directly from the digesters through a sampling port into gas tight collection containers (with a volume of 20 ℓ) which were immediately sealed. During sample collection care was taken that a minimum of CO_2 was lost which would lead to precipitation of minerals before the start of the batch tests. The sealed containers were stored in the laboratory at 20°C for about three days during which time sludge settlement took place. Five litres of liquor was then carefully withdrawn from one container (once more taking care to minimise loss of CO_2) and placed in a batch reactor. Preliminary analysis of the liquor gave soluble (< 0.45 μm) concentrations of Ca = 50 to 60 mg/ℓ, Mg = 20 to 30 mg/ℓ and P_T = 15 to 30 mgP/ℓ. These concentrations were too low to be representative of those in typical BEPR waste activated sludge ADL and so were increased by adding 500 mg of Ca, Mg and P (as Ca, Mg and P from $CaCl_2 \cdot 2H_2O$, $MgCl_2 \cdot 6H_2O$ and K_2HPO_4 respectively) to the 5 ℓ batch volume (i.e. 100 mg/ℓ batch volume of each). *[There were no anaerobic digesters in the Western Cape region treating BEPR waste activated sludge from which SSADL with high concentrations of Mg and P_T could be obtained]*. Immediately after dosing, the liquor was aerated for at least 24 h, but usually up to 56 h to enable the kinetics of ammonia stripping to be observed. Aeration was by means of compressed air passed through a diffuser stone at the bottom of the batch reactor. At frequent intervals, 100 mℓ and 10 mℓ samples were drawn from the batch reactor for Ca, Mg, P_T, C_T, A_T and N_T analysis with the same methods as outlined above for the UASBDL. The pH in the reactor was recorded frequently throughout the batch test and the temperature controlled to 20°C.

Table 6 shows the initial and final values of some of the parameters measured for the three batch tests on UASBDL (Batch tests 16, 17 and 18) and the four batch tests on the SSADL (Batch tests 11, 12, 13 and 14). Detailed results are given in Musvoto et al. (1998).

Model preparation

The model was given as input the eight dissociation constants (pK) and their temperature sensitivities for the 16 forward and reverse dissociation processes for the water, carbonate, phosphate, SCFA and ammonia weak acid/base systems (Tables 2a and 2c in Musvoto et al., 1997) and the 11 stability constants (pK_{ST}) for the 22 forward and reverse dissociation processes for the ion pairs (Tables 1a and 1c above). Also given as input were the solubility product (pK_{SP}) values from the literature for the five minerals identified to precipitate (see Table 7). These pK, pK_{ST} and pK_{SP} values were accepted to be model constants (not changed). With the measured initial conductivity, also given as input and converted internally in the model to an ionic strength value with the formulae given by Loewenthal et al. (1989) (see Table 4a), the input pK, pK_{ST} and pK_{SP} values were internally corrected for ionic strength with the appropriate mono-, di- and tri-valent ion activity coefficients, as indicated in the above mentioned tables. The input pK values were also internally adjusted for temperature; the pK_{ST} and pK_{SP} values could not be adjusted as information on temperature sensitivities for these is not available in the literature. The initial measured total species concentrations (C_T, P_T, N_T, Ca and Mg) and pH were also given as input to the model for the batch tests.

Model calibration - Determination of mineral precipitation and gas stripping rates

Correction for ionic strength in the model is dynamic so that any changes in ionic strength due to precipitation of minerals as the simulation continues, automatically readjusts the pK', pK'_{ST} and pK'_{SP} values. By changing only the precipitation rate constants (K'_{ppt}) for the five minerals and the specific gas stripping rate constants (K_r') for CO_2 and NH_3 (the calibration constants), these seven rate constants were determined by trial and error fitting of theoretical model predictions to the experimental data. The results

TABLE 6

Initial and final concentrations for four aerobic batch tests (11 to 14) on anaerobic digester liquor (SSADL) from a digester treating blended sewage primary sludge and waste activated sludge and three aerobic batch tests (16 to 17) on liquor from a UASB digester treating wine distillery waste (UASBDL)

Parameter	SSADL								UASBDL					
	Batch Test 11		Batch Test 12		Batch Test 13		Batch Test 14		Batch Test 16		Batch Test 17		Batch Test 18	
	Initial	Final*	Initial	Final*	Initial	Final*	Initial	Final*	Initial	Final*	Initial	Final*	Initial	Final*
Calcium (g/m^3)	113	32.1	129	33.6	133	51	83.8	18.6	54.8	23.7	58.6	22.5	55.4	20.0
Magnesium (g/m^3)	125	3.7	116	3.5	128	5.4	128	4.6	81.8	8.0	67.6	6.4	64.6	6.1
Phosphate (gP/m^3)	190	15.9	185	14.6	200	13.3	177	13.3	128	28.8	106	19.8	104	17.0
FSA (gN/m^3)	714	361	770	490	812	353	781	386	128	11.5	128	46.8	127	42.0
Inorganic carbon (gC/m^3)	720	165	700	216	720	126	720	135	820	470	847	490	830	470
pH	6.94	8.77	7.05	8.78	7.09	8.91	7.09	8.93	7.03	9.53	6.95	9.37	6.97	9.48
Duration of test (days; h)	2.25; 54		2.25; 54		2.33; 56		2.25; 54		1.00; 24		1.00; 24		1.00; 24	

*For Ca, Mg and P_T, final concentration is the mean of the last three (SSADL) or two (UASBDL) measurements.

obtained by this "visual" data fitting are listed in Table 7. The Aquasim model includes a parameter estimation facility which searches for selected parameter values between given upper and lower limits that give the best correlation between experimental and theoretical results. To check the "visually" determined precipitation and gas stripping rate constants, these seven rate constants were searched for simultaneously with the parameter estimation facility for each of the four batch tests on SSADL and the three batch tests on UASBDL. The lower and upper limits specified for the seven rate constants were zero and double the visually determined values respectively (all parameter estimation values fell within this range). The rate constants and results from the parameter estimation simulations are given in Table 7. Also given in Table 7 are the concentrations of each mineral precipitated and the mass % these represent in the total concentration of minerals precipitated. Table 8 gives a summary of the *initial concentrations* of Ca, Mg and P_T in the batch tests as well as other parameters cited in the literature which affect the precipitation of the various minerals in wastewaters of this type. It should be noted that these initial concentrations and β ratios change rapidly as the pH increases due to CO_2 expulsion. Therefore, while, for example, $CaCO_3$ is initially undersaturated, it quickly becomes supersaturated and precipitates as the test progresses.

As examples, Figs. 1 to 4 show the measured and predicted results from the parameter estimate simulations for batch tests 16 and 18 on the UASBDL and batch test 11 and 12 on SSADL respectively. It can be seen that a good correlation is obtained between experimental and theoretical model predictions for both liquors. Moreover, visually there is very little discernable difference between Figs. 1 to 4 and the figures (not shown) of the results from the visually determined precipitation and gas stripping rates. A comparison of the predicted results from the visual calibration and parameter estimate simulations can be made from Table 7.

Results and discussion

The following conclusions can be drawn from a comparison of the simulation results for the two liquors (Tables 7 and 8):

Solids most likely to precipitate

The same solids, viz. struvite, ACP, newberyite, $CaCO_3$ and $MgCO_3$, were identified from the literature as most likely to precipitate in both SSADL and UASBDL and on this basis were included in the model. With these precipitants, the consistency between predicted and measured soluble species concentrations (Figs. 1 to 4) indicates that no precipitants of importance have been omitted from the model. From the simulations, in both liquors struvite formed the bulk (80 to 89%) of the total mass of precipitate formed, followed by ACP (3.5 to 14.8%) (Table 7). $MgCO_3$ was predicted to precipitate in the UASBDL, but not in the SSADL. This is because the pH for the UASBDL increased to about 9.5 which is significantly higher than that for the SSADL, where the increase was to about 8.9; the higher pH stimulated $MgCO_3$ precipitation. This is in agreement with the literature where it is noted that at higher pH, $MgCO_3$ is likely to precipitate, but not at lower pH; from the simulations, at the lower pH the concentration of CO_3^{2-} species is too low for the solution to be supersaturated with respect to $MgCO_3$ after most of the struvite has precipitated. In the UASBDL, $MgCO_3$ comprised 3.3 to 4.5% of the total mass of precipitate formed (Table 7). Conversely, $CaCO_3$ was predicted to precipitate in SSADL, but not significantly in UASBDL. This difference in precipitation behaviour between SSADL and UASBDL

ISSN 0378-4738 = Water SA Vol. 26 No. 4 October 2000

TABLE 7

Model input values for the solubility products of the five minerals identified to precipitate in the seven aeration batch tests on the SSADL and UASBDL and model simulation results giving the mineral precipitation and gas stripping rate constants determined by trial and error visual correlation and Aquasim parameter estimation.

Test		Visual estimation results								Aquasim Parameter estimation results							
		Str'vite	Nwb'ite	ACP	$CaCO_3$	$MgCO_3$	O_2	CO_2	NH_3	Str'vite	Nwb'ite	ACP	$CaCO_3$	$MgCO_3$	O_2	CO_2	NH_3
	pK_{SP}	13.16	5.8	26.0	6.45	7.00	$K'_{La,O2}$	$K'_{La,CO2}$	$K'_{La,NH3}$	13.16	5.8	26.0	6.45	7.00	$K'_{La,O2}$	$K'_{La,CO2}$	$K'_{La,NH3}$
	Refs*[1]	(1)	(1)	(2)	(3)	(4)	-	-	-	(1)	(1)	(2)	(3)	(4)	-	-	-
BT 11 SSADL μ=0.16 54h	Rate*[2]	300	0.05	150	50	50	300	273	1.1	177	0.01	241	14	13	286	260	1.1
	Conc*[3]	1236	3.8	140	58	0	-	580	239	1209	1.3	154	51	<0.1	-	580	241
	%	88	0.3	10	4.1	0	-	-	-	85	0.1	11	3.6	0	-	-	-
BT 12 SSADL μ=0.17 54h	Rate*[2]	300	0.05	150	50	50	225	204	1.2	293	0.06	168	46	57	225	205	1.2
	Conc*[3]	1140	2.8	170	46	0	-	545	226	1128	4.0	175	70	<0.1	-	545	228
	%	84	0.2	12.5	3.4	0	-	-	-	82	0.3	13	5.1	0	-	-	-
BT 13 SSADL μ=0.18 54h	Rate*[2]	300	0.05	150	2[4]	50	550	500	1.05	357	0.01	249	0.6	15	510	464	1.35
	Conc*[3]	1250	2.8	160	43	0	-	618	330	1237	1.0	198	23	<0.1	-	619	334
	%	85	0.2	11.0	3.0	0	-	-	-	85	0.1	14	1.6	0	-	-	-
BT 14 SSADL μ=0.16 54h	Rate*[2]	300	0.05	150	50[4]	50	600	545	0.9	267	0.07	165	68	68	588	538	1.0
	Conc*[3]	1270	2.6	50	98	0	-	596	292	1247	3.7	66	91	0.95	-	596	292
	%	89	0.2	3.5	6.9	0	-	-	-	89	0.3	4.7	6.5	0	-	-	-
BT 16 UASBDL μ=0.08 24h	Rate*[2]	3000	0.05	350	0.5	50	670	610	1.92	2406	0	388	0.3	39	619	563	1.98
	Conc*[3]	677	2.1	91[5]	<0.1	30	-	389	49	675	0	91	0.5	31	-	389	49
	%	84	0.3	11.4	0	3.8	-	-	-	85	0	11	0.1	3.9	-	-	-
BT 17 UASBDL μ=0.08 24h	Rate*[2]	3000	0.05	350	0.5	50	400	365	2.5	2309	0	371	0.3	39	453	412	2.5
	Conc*[3]	532	1.2	98	<0.1	30	-	389	49	530	0	98	0.5	31	-	389	49
	%	80	0.2	14.8	0	4.5	-	-	-	80	0	15	0.1	4.7	-	-	-
BT 18 UASBDL μ=0.08 24h	Rate*[2]	3000	0.05	350	0.5	50	670	610	1.92	1815	0	385	0.3	48	581	529	2.2
	Conc*[3]	528	0	92	<0.1	21[5]	-	389	49	504	0	93	0.4	29	-	389	49
	%	82	0	14.4	0	3.3	-	-	-	80	0	15	0.1	4.6	-	-	-

*[1] References for pK_{SP} values: (1) Struvite and Newberyite - JESS - Murray and May (1996); (2) ACP - Butler (1964); (3) $CaCO_3$ - Merrill and Jorden (1975); (4) $MgCO_3$ - Not from any specific reference - selected 7.00 from the range reported by Mamais et al. (1994) - see Table 2.

*[2] Rates in per day.

*[3] Mineral precipitant concentrations in mg/ℓ, CO_2 in mgC/ℓ and NH_3 in mgN/ℓ.

*[4] Correct as given here - interchanged in Musvoto et al. (2000).

*[5] Correct as given here - incorrectly reported as 9.1 and 2.1 in Musvoto et al. (2000).

TABLE 8
Summary of some of the concentrations and parameters at the start of the batch tests (initial, i) that affect the precipitation of minerals for batch tests on SSADL and UASBDL

Batch test No.	ADL Type	Mg_i g/m³	Ca_i g/m³	P_{Ti} gP/m³	Mg_i mol/ℓ	Ca_i mol/ℓ	P_{Ti} mol/ℓ	Mg/Ca molar	Mg/P molar	Ca/P molar	β_{Ni}	β_{Si}	β_{Ni}/β_{Si}	β_{CaCO3i}
11	SSADL	125	113	190	0.0052	0.0028	0.0061	1.86	0.85	0.46	4.4	6.1	0.72	0.08
12	SSADL	116	129	152	0.0048	0.0032	0.0049	1.5	0.98	0.65	4.7	9.0	0.52	0.12
13	SSADL	128	133	200	0.0053	0.0033	0.0065	1.61	0.82	0.51	6.3	16.3	0.39	0.14
14	SSADL	128	83.8	177	0.0053	0.0021	0.0057	2.52	0.93	0.37	5.5	12.0	0.46	0.09
16	UASBDL	81.8	54.8	128	0.00034	0.0014	0.0041	2.43	0.83	0.34	2.4	0.9	2.7	0.05
17	UASBDL	67.6	58.6	106	0.0028	0.0015	0.0034	1.87	0.82	0.44	1.4	0.35	4.0	0.05
18	UASBDL	64.6	55.4	104	0.0027	0.0014	0.0034	1.93	0.79	0.41	1.4	0.35	4.0	0.05

Note: 1. β_{Ni}, β_{Si}, and β_{CaCO3i} are the initial supersaturation for newberyite, struvite and $CaCO_3$ respectively. Initial supersaturation is defined as the ratio of the initial ionic product to the solubility product e.g. for $CaCO_3$, $\beta_{CaCO3i} = (Ca^{2+}{}_i)(CO_3{}^{2-}{}_i)/K_{spCaCO3}$
2. Subscripts "T" = total ortho-phosphate species, and "i" = initial.

for $CaCO_3$ could only be taken into account in the simulations by significantly reducing the precipitation rate for the UASBDL batch tests (see below). In the SSADL, $CaCO_3$ comprised 3.0 to 6.9% of the total mass of precipitate formed. Newberyite was predicted to precipitate in small amounts from both liquors in the visual calibration simulations whereas in the parameter estimation simulations it was predicted to precipitate only in the SSADL; however, in all simulations it comprised only < 0.3% of the precipitate mass formed (Table 7). From information in the literature, this is expected because the pH, initial molar concentrations and the degrees of supersaturation for newberyite and struvite present during aeration favour the precipitation of struvite over newberyite, i.e. newberyite precipitates at pH < 6.0, P concentrations > 0.01M and $\beta_{Ni}/\beta_{Si} > 4$ (Abbona et al., 1982).

Solubility products (pK_{SP})

For each of the five minerals that precipitated, the pK_{SP} values were model constants (not changed) and were the same for both the SSADL and UASBDL (Table 7). All are within the range of accepted literature values (Table 7) commonly used in equilibrium based water chemistry (see Table 2).

Specific rate constants for precipitation (K'_{ppt})

From the parameter estimation results (Table 7), in the UASBDL the K'_{ppt} for struvite and ACP, which together make up >95% of the precipitate mass, varied from 1 815 to 2 406/d and 371 to 388/d respectively. The K'_{ppt} for Newberyite and $CaCO_3$ were the same in all three batch tests at 0/d and 0.3/d respectively. The K'_{ppt} for $MgCO_3$ varied from 39 to 48/d. Struvite and ACP precipitation were complete in three and eight minutes respectively. This can be seen in Fig. 5 which shows the concentration of mineral precipitated with time for Batch Test 16 on UASBDL (parameter estimate prediction). The batch tests were continued for at least 24 h to observe also the ammonia stripping rate (see below).

From the parameter estimation results (Table 7), in the SSADL the K'_{ppt} for struvite and ACP varied from 177 to 357 /d and 165 to 249/d respectively. The K'_{ppt} for Newberyite was very low and varied from 0.01 to 0.07 /d. The K'_{ppt} for $CaCO_3$ varied between 14 and 68/d with one very low value of 0.6 /d for Batch Test 13. The K'_{ppt} for $MgCO_3$ varied between 13 and 68 /d (however, the very small amount of $MgCO_3$ precipitated, < 1mg/ℓ, makes accurate estimation of this rate difficult). The reason for the very low K'_{ppt} for $CaCO_3$ in Batch Test 13 could not be established. Initially from the visual fit simulations it was thought that Mg interference caused the rate to be so low (Musvoto et al., 2000), but this was due to incorrectly transposing this low rate with that of Batch Test 14. Batch Test 14 had the highest initial Mg/Ca ratio (Table 8) and the precipitation rate of $CaCO_3$ is known to decrease with increasing Mg/Ca ratio (Benjamin et al., 1977), an effect exacerbated by PO_4 at Mg/P molar ratios of 1.5 to 2 (Benjamin et al., 1977; Danen-Louwerse et al., 1995). However, after scrutiny of the results, it was found that Batch Test 14 had the highest K'_{ppt} for $CaCO_3$ of 68 /d (Table 7) and that Batch Test 13 was the one with the low K'_{ppt} for $CaCO_3$ even though it had lower Mg/Ca and Mg/P ratios than Batch Test 14. The low K'_{ppt} for $CaCO_3$ in Batch Test 13 therefore could not be due to the effect of Mg or P.

For some reason that could not be determined, in both the visual fit and parameter estimation simulations Batch Test 13 with the very low K'_{ppt} for $CaCO_3$ differs from the other three tests on SSADL. The visually calibrated and parameter estimation simulation results for Batch Test 13 are shown in Figs. 6 and 7 respectively. Because in the visual calibration a good correlation with pH was emphasised (Fig. 6), the correlation for pH is good but for the FSA, Ca and C_T the correlation is not so good. In the parameter estimate simulations (Fig. 7), this bias towards a good fit for pH was absent and the correlation between the predicted and observed results is improved for FSA, Ca and C_T, but the pH is consistently under predicted. As is evident above, this lack of fit with all the measured data is absent in the other 6 batch tests.

Comparison of specific precipitation rates in UASBDL and SSADL

The specific precipitation rate constants (K'_{ppt}) found for struvite, ACP and $CaCO_3$ differ significantly between the SSADL and UASBDL (Table 7). The rates for struvite and ACP in both the visual and parameter estimation simulations are much higher in the UASBDL than in the SSADL. Conversely, in both sets of simulations the rate for $CaCO_3$ is lower for the UASBDL than for SSADL. The rates for Newberyite and $MgCO_3$ were similar in the UASBDL and

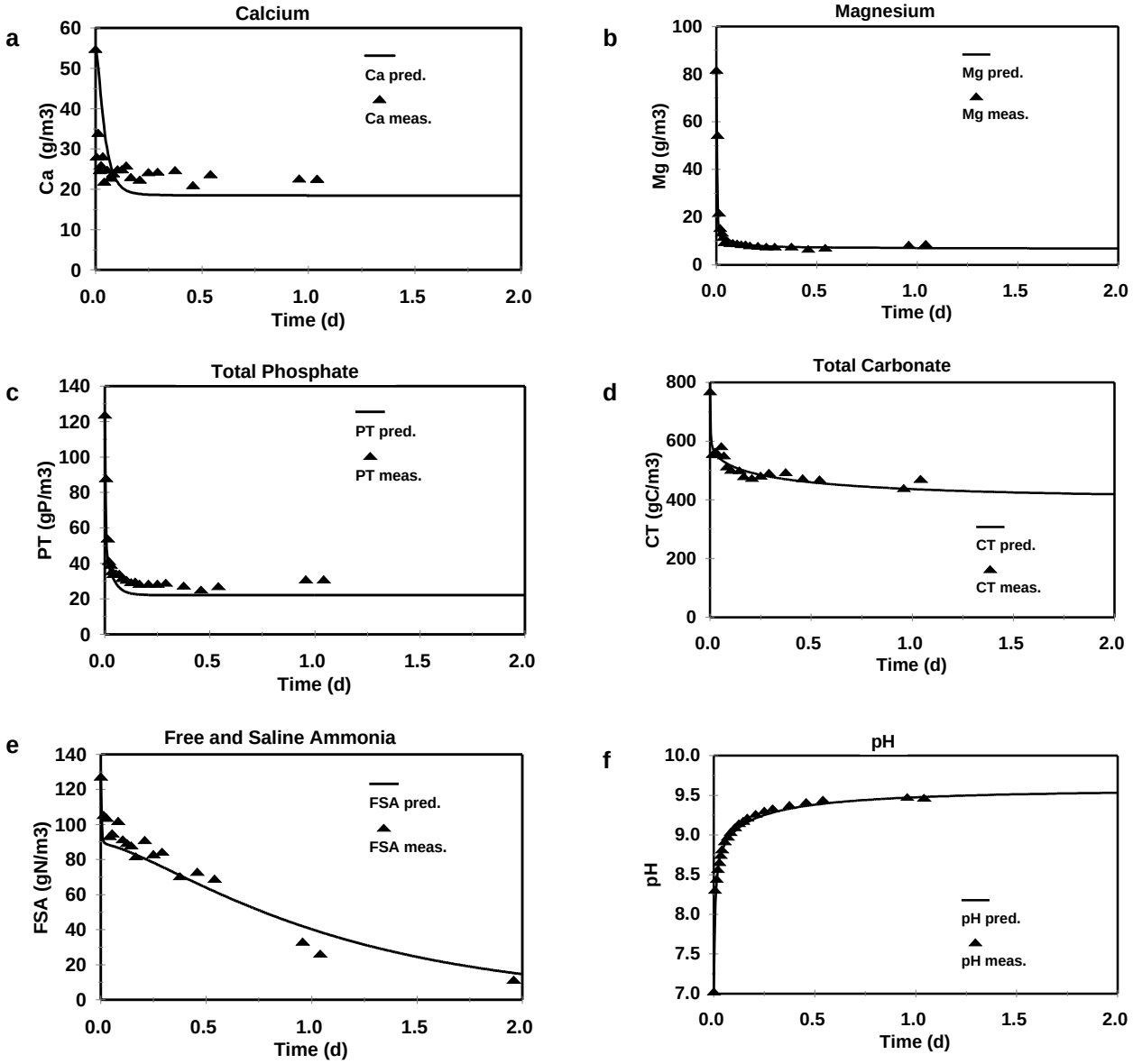

Figure 1

Predicted (parameter estimate results) and measured soluble concentrations for calcium (Ca, Fig. 1a, top left), magnesium (Mg, Fig. 1b, top right), total phosphate species (P_T, Fig. 1c, middle left), total carbonate species (C_T, Fig. 1d, middle right), free and saline ammonia (FSA, Fig. 1e bottom left) and pH (Fig. 1f, bottom right) for aeration Batch Test 16 on anaerobic digester liquor from Stellenbosch Farmers' Winery (Wellington, South Africa) spent wine UASB digester.

SSADL, viz. 0.05/d and 50/d respectively for visual simulations and between 0 and 0.07/d and 13 and 68/d respectively for parameter estimation simulations. With regard to the K'_{ppt} for struvite and ACP, it is most likely that these differences are due to inhibition of the precipitation process through "poisoning" of the crystal growth sites. The presence of even small amounts of foreign organic and inorganic constituents, trace quantities of surfactants and other materials are known to alter significantly the growth rate of crystals and their morphology (Stumm and Morgan, 1981). The SSADL contained considerably more particulate organics than the UASBDL, which most likely acted as inhibitors (rather than providing more seed material surface area) and probably is the reason for the slower rates of precipitation of struvite and ACP in the SSADL than in the UASBDL.

With regard to the precipitation rate of $CaCO_3$, from the literature this is particularly sensitive to and inhibited by the presence of dissolved organic matter, polyphosphates, polyphenols, phosphoric acid derivatives, fulvic acid, magnesium, organic and inorganic phosphate and iron. Fe^{2+} is known to be the strongest inhibitor, reducing the $CaCO_3$ growth rate even at very low concentrations (Droomgoole and Walter, 1990). The inhibition by inorganic P depends on both the initial concentration and the initial degree of supersaturation of $CaCO_3$. The phosphate concentration in solution does not affect the kinetics of precipitation once crystal growth has started, but generally the rate of precipitation is lower if the initial supersaturation of $CaCO_3$ is lower (House, 1987). In the experiments, the initial Mg/Ca and Mg/PO_4-P ratios are not significantly different in the two liquors, though the initial Mg/Ca ratio tends to be higher in the UASBDL (Table 8). The initial $CaCO_3$ saturation is lower in the UASBDL than in SSADL, but initially both are strongly undersaturated with $CaCO_3$. Because in the batch test several minerals are precipitating and pH is rising, the

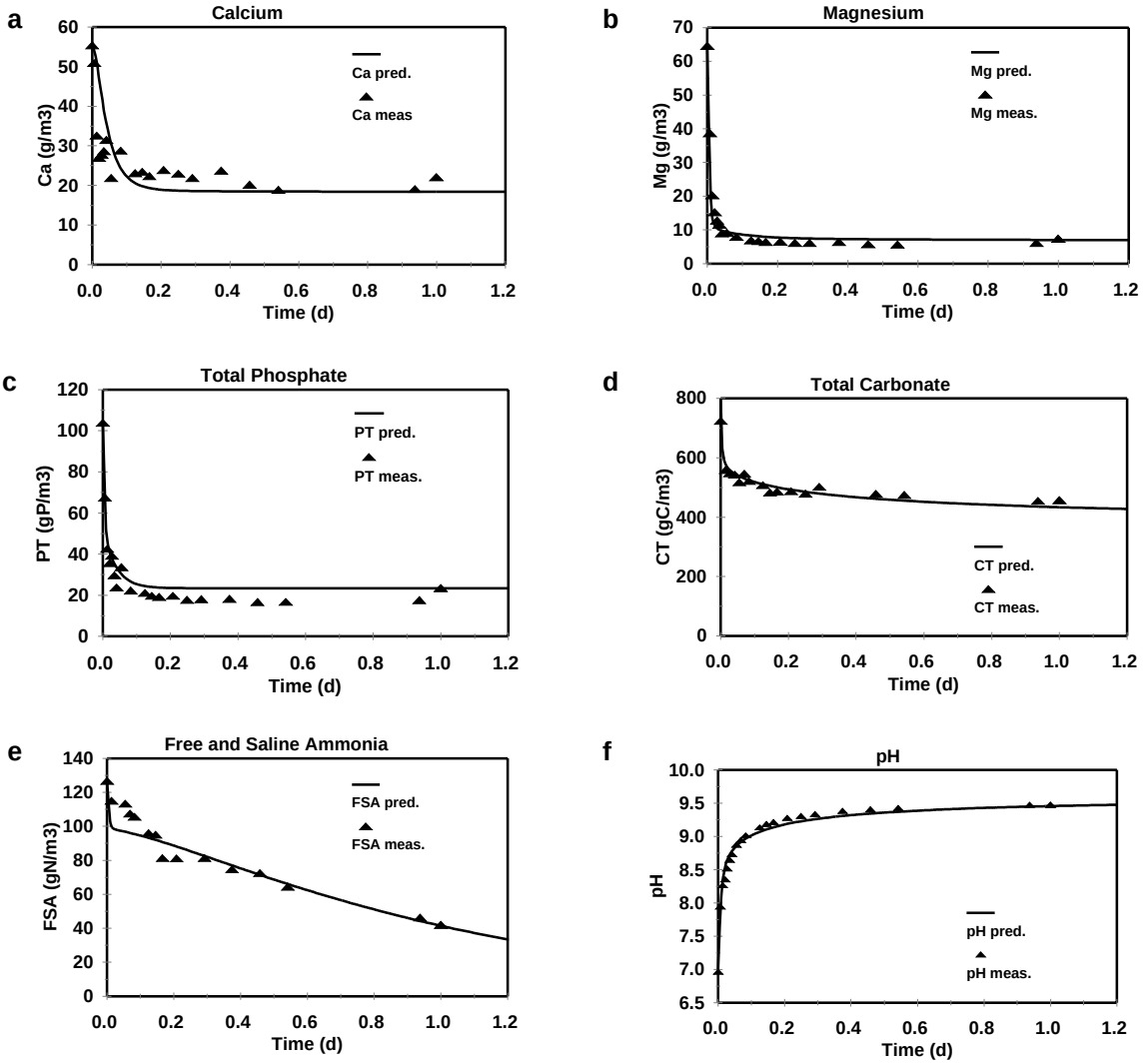

Figure 2

Predicted (parameter estimate results) and measured soluble concentrations for calcium (Ca, Fig. 2a, top left), magnesium (Mg, Fig. 2b, top right), total phosphate species (P_T, Fig. 2c, middle left), total carbonate species (C_T, Fig. 2d, middle right), free and saline ammonia (FSA, Fig. 2e bottom left) and pH (Fig. 2f, bottom right) for aeration Batch Test 18 on anaerobic digester liquor from Stellenbosch Farmers' Winery (Wellington, South Africa) spent wine UASB digester.

relative ratios of the species concentrations and the saturation state change with time. Because struvite precipitates so rapidly and ACP more slowly, the P_T and Mg concentrations decrease very quickly, but the Ca concentration more slowly. This, with the rising pH, causes $CaCO_3$ to become supersaturated several minutes into the test. Therefore, by the time $CaCO_3$ starts precipitating, the Mg and P_T concentrations are already low. Under these conditions, it is difficult to assess the significance of the effect of initial condition parameters (concentration and β ratios such as in Table 8) on the precipitation rates.

Although the filtered COD concentration (which is an indication of soluble organics) was not measured for each batch test, measurements on a few samples showed a soluble concentration of 900 mg/ℓ for SSADL and 980 mg/ℓ for UASBDL. Measurements of Fe indicated low concentrations (0.2 to 0.7mg/ℓ) and that the concentrations did not differ significantly between SSADL and UASBDL; accordingly, this cannot account for the difference in $CaCO_3$ precipitation rates between the two liquors. The presence of compounds such as pyrophosphates, polyphenols and fulvic acid, which are known to inhibit $CaCO_3$ precipitation, were not determined in the two liquors. It therefore appears that the lower precipitation rate constant for $CaCO_3$ in the UASBDL may be due to: (i) higher concentrations of inhibiting compounds like pyrophosphates, (ii) a lower initial $CaCO_3$ β ratio and possibly, though unlikely, (iii) dissolved organic substances because the filtered COD of the UASBDL is slightly higher than the SSADL. Because all these effects are not taken into account directly in the model, they are reflected by a change in the specific precipitation rate constant. However, it is not possible to identify definitively the cause for the difference in $CaCO_3$ precipitation rates between the two liquors.

Gas stripping

The specific rates for gas stripping for both CO_2 and NH_3 differed for each individual batch test (Table 7). This is not unexpected because the aeration conditions (gas flow rates, mixing, solids, etc.) differed in each batch test. With the clarity of hindsight, the

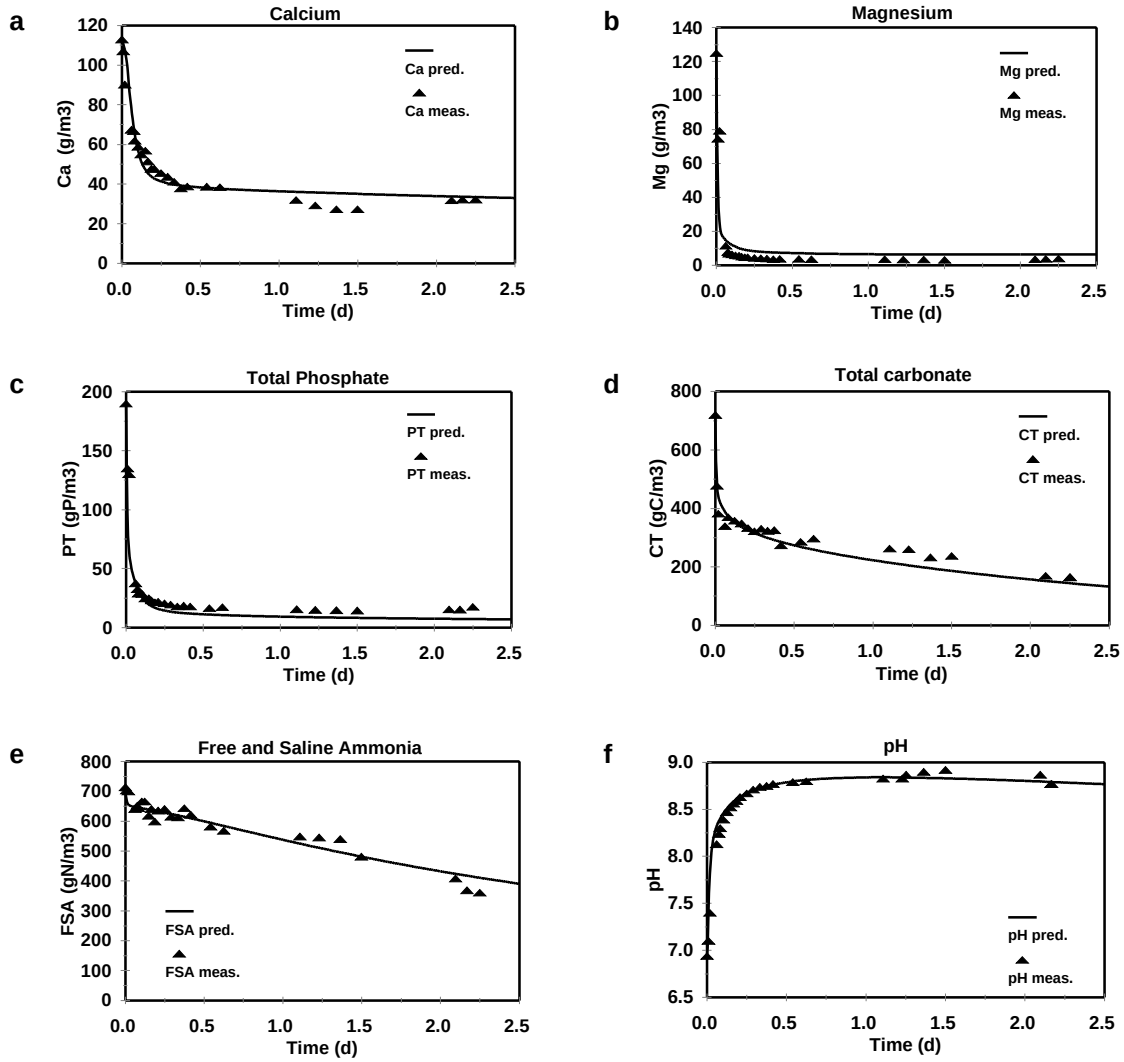

Figure 3

Predicted (parameter estimate results) and measured soluble concentrations for calcium (Ca, Fig. 3a, top left), magnesium (Mg, Fig. 3b, top right), total phosphate species (P_T, Fig. 3c, middle left), total carbonate species (C_T, Fig. 3d, middle right), free and saline ammonia (FSA, Fig. 3e bottom left) and pH (Fig. 3f, bottom right) for aeration Batch Test 11 on anaerobic digester liquor from Cape Flats WWTP (Cape Town, South Africa) digester treating primary and waste activated sludge.

aeration rates in the batch tests should have been controlled to be the same for all the batch tests, which would have eliminated the specific gas stripping rate as a calibration constant for each batch test.

Comparison of CO_2 and NH_3 stripping rates

The stripping rate for CO_2 is much higher, by two orders of magnitude, than that for NH_3. This is in agreement with the literature where it is evident that the volatility of NH_3 is much lower than that for CO_2. This is reflected in the value for the dimensionless Henry's law constant (H_C). For NH_3, $H_C = 0.011$ whereas for CO_2, $H_C = 0.95$ (Loewenthal et al., 1986; Katehis et al., 1998). In the batch tests, the pH was raised by stripping CO_2. Because this process is relatively slow, the mineral precipitation rates may have been influenced by the pH rise rate. The effect of the gas stripping rate on the mineral precipitation rates was not examined in this investigation. In future work it is intended to measure the mineral precipitation rates in batch tests with lime or NaOH addition to rapidly increased the pH without aeration or with delayed aeration at controlled rates, to examine the effect of this on the mineral precipitation rates.

Conclusion

The three-phase physical-chemical kinetic model developed for the carbonate system (Musvoto et al., 1997) is extended to include the phosphate, ammonia and short chain fatty acid weak acid/base systems in three phases with multi-mineral precipitation and multi-gas stripping. The specific kinetic model developed is to simulate the physical-chemical reactions which occur in the aeration treatment of anaerobic digester liquors (ADL). The processes that occur under these conditions are the dissociation of the weak acid/bases, precipitation of solids (struvite, newberyite, amorphous calcium phosphate, magnesium and calcium carbonate) and stripping of CO_2 and NH_3 gases. Ion pairing effects are also included in the model because the ionic strength of the liquors tested was greater than 0.025.

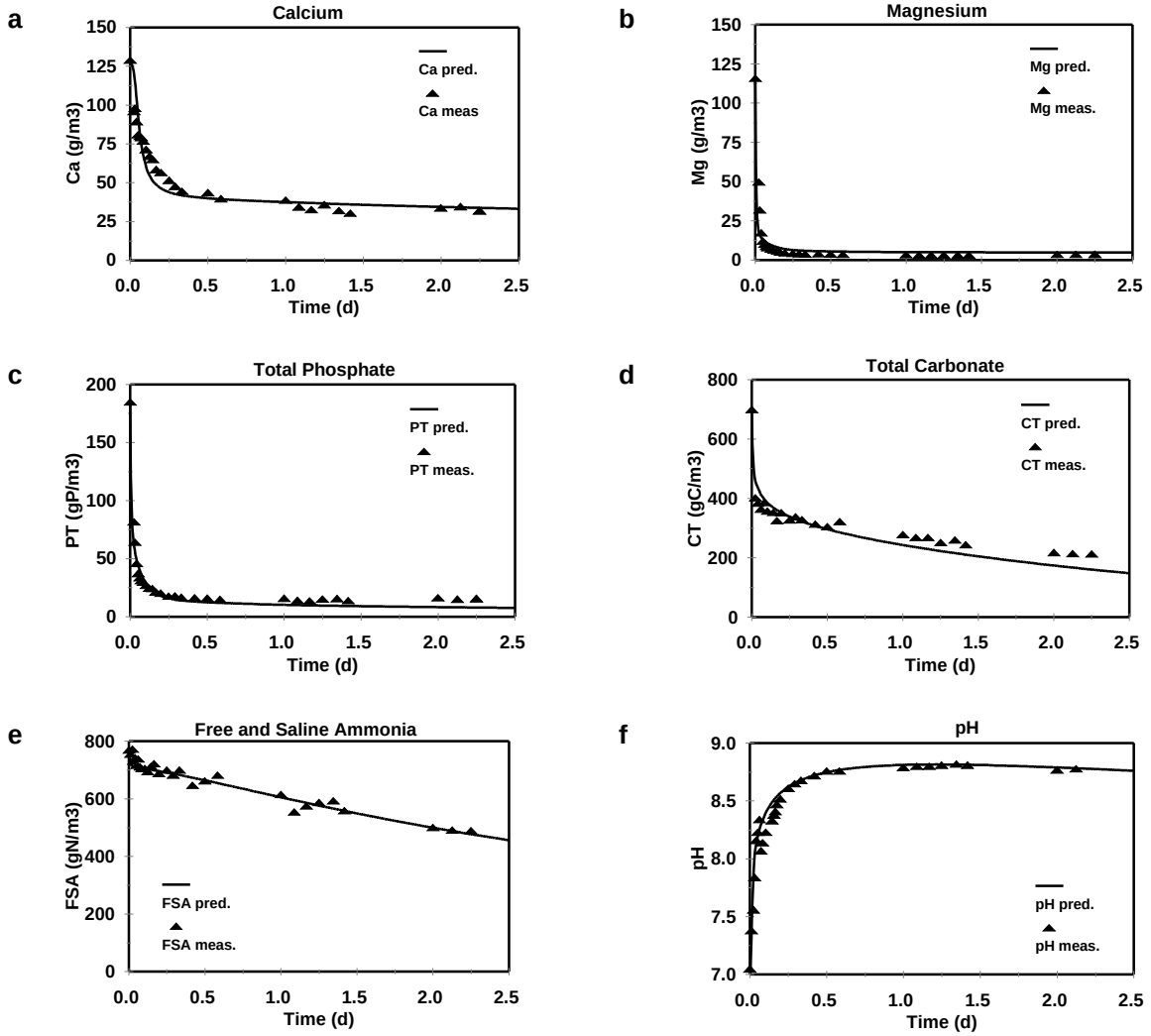

Figure 4

Predicted (parameter estimate results) and measured soluble concentrations for calcium (Ca, Fig. 4a, top left), magnesium (Mg, Fig. 4b, top right), total phosphate species (P_T, Fig. 4c, middle left), total carbonate species (C_T, Fig 4d, middle right), free and saline ammonia (FSA, Fig 4e bottom left) and pH (Fig 4f, bottom right) for aeration Batch Test 12 on anaerobic digester liquor from Cape Flats WWTP (Cape Town, South Africa) digester treating primary and waste activated sludge.

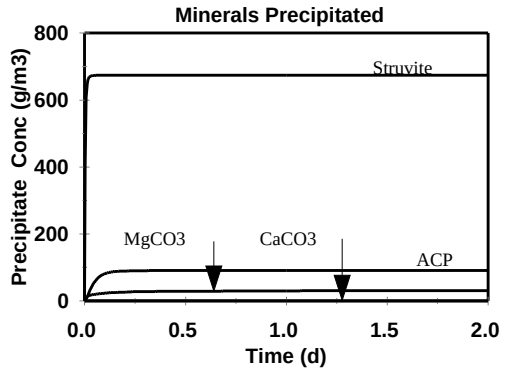

Figure 5

Predicted (parameter estimate results) concentrations of struvite, amorphous calcium phosphate (ACP), $MgCO_3$ and $CaCO_3$ precipitated with time in aeration Batch Test 16 on anaerobic digester liquor from Stellenbosch Farmers' Winery (Wellington, South Africa) spent wine UASB digester. Newberyite ($MgHPO_4$) too low to be included.

In the kinetic model the dissociation constants, ion pair stability constants and mineral solubility products were regarded as model constants and were not changed (except for ionic strength and temperature adjustments). The specific precipitation rates of the minerals and the specific stripping rates of the gases were regarded as calibration constants and changed to fit predicted to experimental results. The calibration constants are important when simulating time dependent experimental results and when simulating the final equilibrium condition for a solution with precipitation of multiple minerals that compete for common species (e.g. ACP and $CaCO_3$ competing for Ca species). In these latter solutions the final equilibrium condition may be influenced by the relative rates of precipitation of the competing precipitating minerals. For time independent simulations with non-competing minerals precipitating, when comparing predicted with observed results of only the final steady state conditions, only the model constants are important.

To check the performance of the model with a single precipitating mineral under time independent conditions, predicted results were compared with the Struvite 3.1 equilibrium based computer

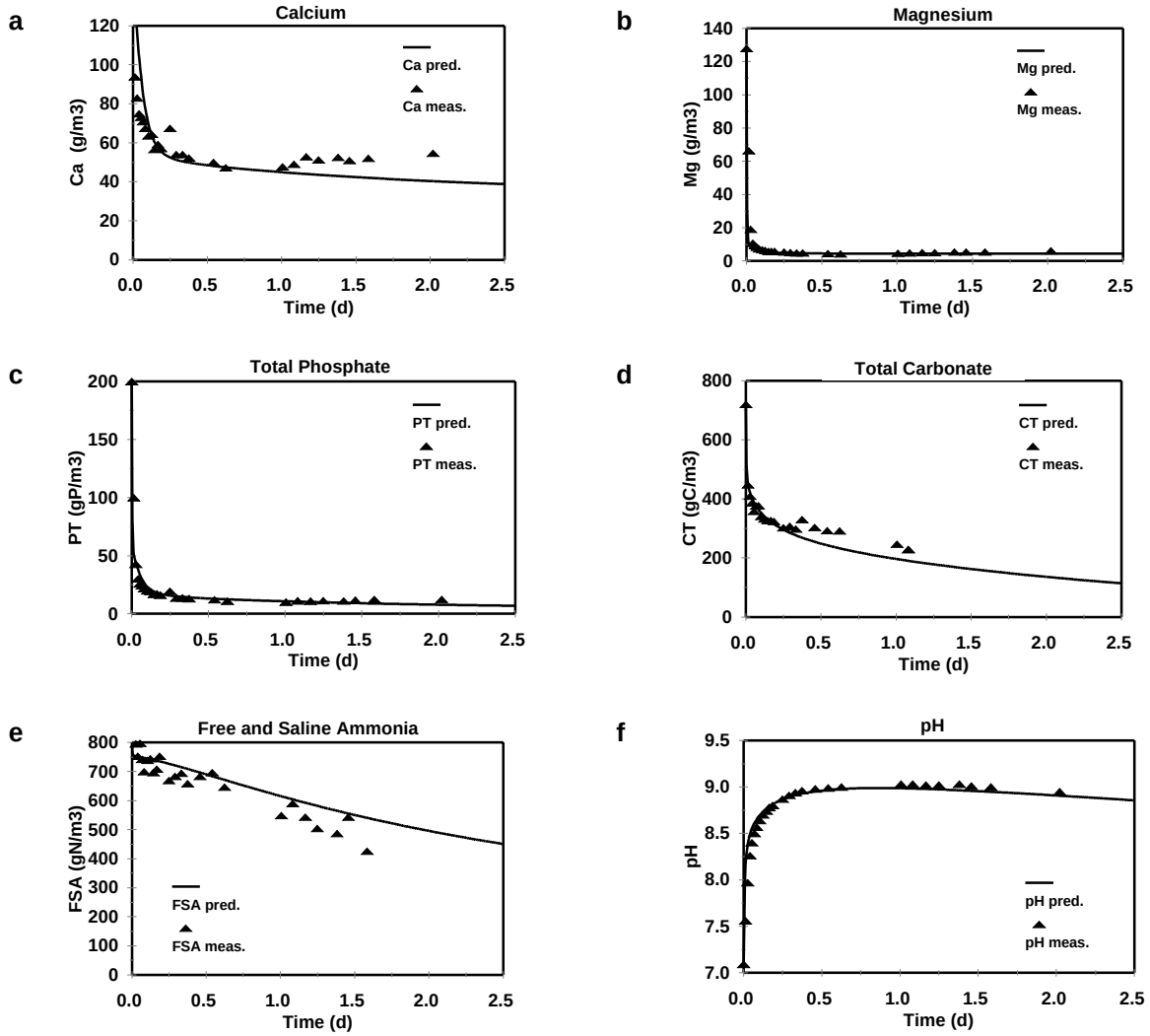

Figure 6

Predicted (visual calibration results) and measured soluble concentrations for calcium (Ca, Fig. 6a, top left), magnesium (Mg, Fig. 6b, top right), total phosphate species (P_T, Fig. 6c, middle left), total carbonate species (C_T, Fig. 6d, middle right), free and saline ammonia (FSA, Fig. 6e bottom left) and pH (Fig. 6f, bottom right) for aeration Batch Test 13 on anaerobic digester liquor from Cape Flats WWTP (Cape Town, South Africa) digester treating primary and waste activated sludge.

program of Loewenthal and Morrison (1997). Since in this situation only a single mineral is precipitating (struvite), only the model constants are of importance. From this comparison it was concluded that the kinetic model can accurately predict equilibrium conditions for single mineral precipitation. To check the performance of the model for multiple mineral precipitation, the experimental results of Ferguson and McCarty (1971) were simulated. In the experiments of Ferguson and McCarty, although only initial and final conditions are available, because multiple competing minerals are precipitating both the model and calibration constants are of importance. From these simulations it was concluded that the model performed well and was sufficiently robust and stable to simulate multiple mineral precipitation.

To validate the time dependent performance of the model and determine the calibration constants, batch experiments were conducted by aerating two anaerobic digester liquors (ADL), viz. three batch tests on liquor from a spent wine UASB digester (UASBDL) and four batch tests on liquor from an anaerobic digester treating a blended primary sludge and waste activated sludge (SSADL). In these batch tests, Ca, Mg, PO_4-P (P_T), inorganic C (C_T, via the H_2CO_3* Alk), free and saline ammonia (FSA, N_T) and pH were measured over 24 to 54 h. After establishing the minerals most likely to precipitate viz. struvite ($MgNH_4PO_4$), newberyite ($MgHPO_4$), amorphous calcium phosphate [ACP, $Ca_3(PO_4)_2$], $CaCO_3$ and $MgCO_3$ and their solubility products from the literature, the specific precipitation and gas stripping rate constants were determined by trial and error visual fitting of predicted results to the experimental data and a parameter estimation facility which searches for the calibration constants that minimise the error between the model predictions and experimental results. A good correlation was obtained between model predictions and experimental results with both methods for six of the seven batch tests and while the second method may be superior, visually there was no discernable difference between the predicted results of the two methods. The good correlation indicated that no mineral that precipitated significantly in the ADL was omitted from the model.

The same minerals were found to precipitate in the two liquors and in similar proportions, viz. in decreasing proportion of precipitate mass formed struvite ($MgNH_4PO_4$) (82 to 89%), amorphous calcium phosphate (ACP) (5 to 15%), calcium carbonate ($CaCO_3$)

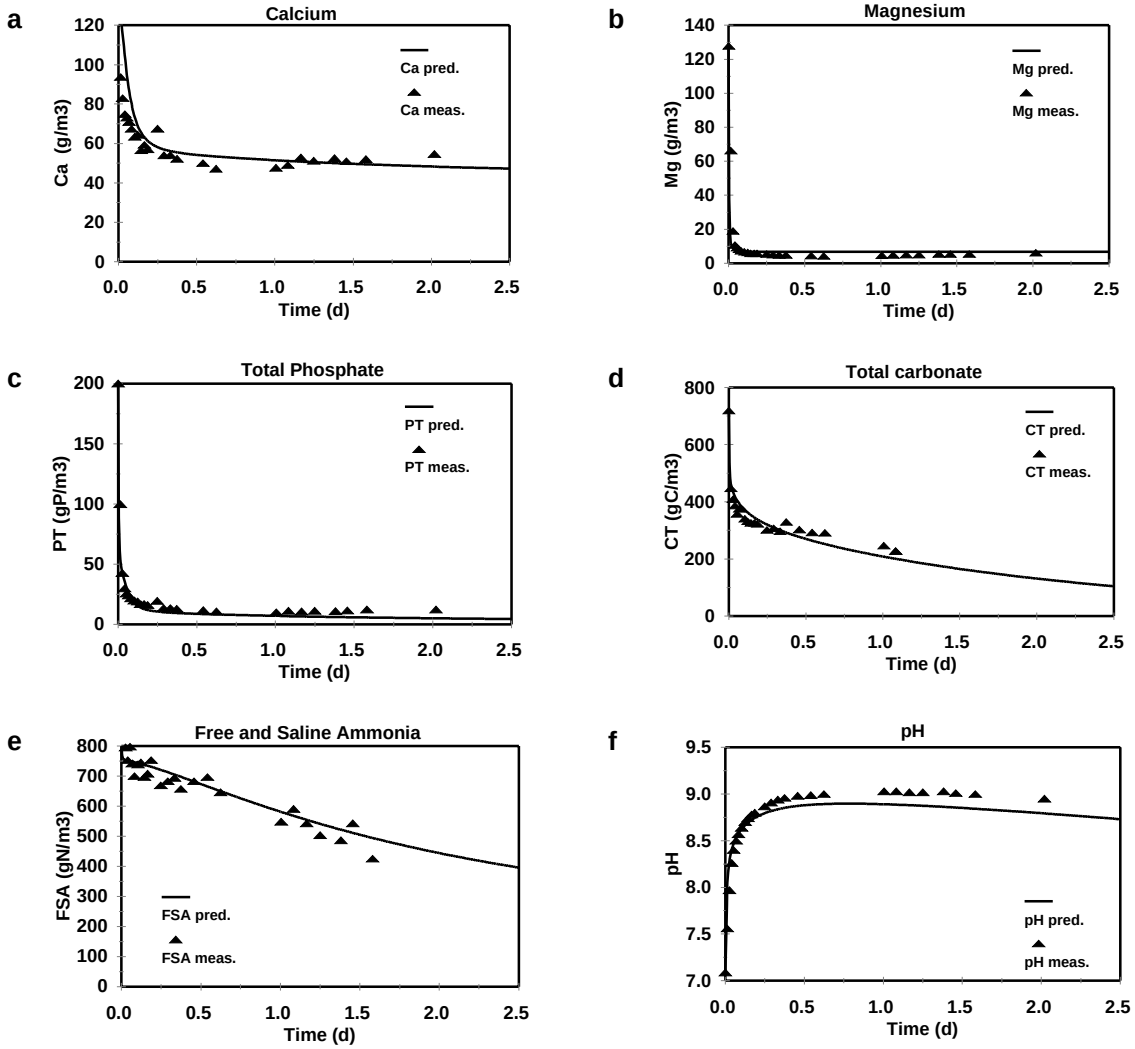

Figure 7

Predicted (parameter estimate results) and measured soluble concentrations for calcium (Ca, Fig. 7a, top left), magnesium (Mg, Fig. 7b, top right), total phosphate species (P_T, Fig. 7c, middle left), total carbonate species (C_T, Fig. 7d, middle right), free and saline ammonia (FSA, Fig. 7e bottom left) and pH (Fig. 7f, bottom right) for aeration Batch Test 13 on anaerobic digester liquor from Cape Flats WWTP (Cape Town, South Africa) digester treating primary and waste activated sludge.

(0 to 6%), magnesium carbonate ($MgCO_3$) (0 to 5%) and newberyite ($MgHPO_4$) (0.1 to 0.3%). Unfortunately no experimental tests were conducted to measure the concentration of precipitate formed. Comparing the mineral precipitation rates in the UASBDL and SSADL, it was found that the rates of struvite and ACP precipitation were 9 and 2 times faster respectively in the UASBDL than in the SSADL; in contrast, the rate of $CaCO_3$ precipitation was 140 times faster in the SSADL than in the UASBDL; the rates of $MgCO_3$ and $MgHPO_4$ precipitation were approximately the same in both liquors. No meaningful comparison could be made for the gas stripping rates because the aeration rate was different in each batch test and these were not measured. This is the weakest part of the batch tests and is, in hindsight, an omission; if the aeration rate had been measured, a comparison could have been made between the airflow rate and CO_2 and NH_3 gas stripping rates.

From the simulations it is evident that the kinetic model offers considerable advantages over equilibrium based models. Not only can it predict time dependent data, but also it can predict the final equilibrium state for situations with precipitation of multiple minerals which compete for the same species - equilibrium models are not capable of predicting either situation. Further, the kinetic modelling approach also allows the determination of the specific precipitation rates for a number of minerals simultaneously in an integrated manner from a single batch test. However, it should be noted that the kinetic model developed here is restricted to the precipitation of minerals and does not consider dissolution; for the tests considered dissolution was not significant compared to the precipitation. For situations where dissolution is significant, the kinetic model will predict neither the time dependent behaviour nor the final equilibrium state correctly. Attempts to include separate processes for dissolution in the model caused instability in model simulations in Aquasim. This aspect requires further investigation.

The three-phase kinetic based weak acid/base chemistry model, and the approach on which it is based, is proving to be a useful tool for research into and design of wastewater treatment systems in which several weak acid/bases influence the behaviour. For research, the model helps to focus attention on issues not obvious from direct experiment and allows determination of mineral precipitation rates for a particular wastewater from a single batch test. Once calibrated with the precipitation (and gas stripping if in-

cluded) rates, this kind of model can be used to predict the performance of different treatment systems to identify for investigation those that appear technically and economically viable. In further work, this modelling approach will be extended to include biological processes, such as those of anaerobic digestion or biological nutrient removal activated sludge. This will allow modelling of biological treatment systems together with the mixed weak acid/base chemical systems within which the biological processes operate or combined biological/chemical systems such as simultaneous chemical/biological P removal.

Acknowledgements

The authors wish to thank the reviewers for their careful scrutiny of the manuscript. Their astute and valuable comments were very helpful in the revision of the manuscript and significantly contributed to an improved final paper. This research was supported financially by the Water Research Commission, National Research Foundation and the University of Cape Town and is published with their permission.

References

ABBONA F, LÜNDAGER MADSEN HE and BOISTELLE R (1982) Crystallization of two magnesium phosphates, struvite and newberyite: Effect of pH and concentration. *J. Cryst. Growth* **57** (1) 6-14.

ABBONA F, LÜNDAGER MADSEN HE and BOISTELLE R (1986) The initial phases of calcium and magnesium phosphates precipitated from solutions of high to medium concentration. *J. Cryst. Growth* **74** 581-590.

ABBONA F, LÜNDAGER MADSEN HE and BOISTELLE R (1988) The final phases of calcium and magnesium phosphates precipitated from solutions of high to medium concentration. *J. Cryst. Growth* **89** 592-602.

ARVIN E (1983) Observations supporting phosphate removal by biologically mediated chemical precipitation - A review. *Water Sci. Technol.* **15** 43-63.

BATTISTONI P, FAVA G, PAVAN P, MUSACCO A and CECCHI F (1997) Phosphate removal in anaerobic liquors by struvite crystallization without addition of chemicals: Preliminary results. *Water Res.* **31**(11) 2925-2929.

BENJAMIN L, LOEWENTHAL RE and MARAIS GvR (1977) Calcium carbonate precipitation kinetics Part 2 - Effects of magnesium. *Water SA* **3** (3) 155-165.

BETTS F, BLUMENTHAL NC and POSNER AS (1981) Bone mineralization. *J. Cryst. Growth* **53** 63-73.

BLUMENTHAL NC, BETTS F and POSNER AS (1977) Stabilisation of amorphous calcium phosphate by Mg and ATP. *Calcif. Tiss. Res.* **23** 245-250.

BORGERDING J (1972) Phosphate deposits in digestion systems. *J. WPCF* **44** (5) 813-819.

BUTLER JN (1964) *Ionic Equilibrium - A Mathematical Approach*. Addison-Wesley Publishing Co. Inc., Reading, Massachusetts.

CHUGHTAI A, MARSHALL R and NANCOLLAS GH (1968) Complexes in calcium phosphate solutions. *J. Phys. Chem*. **72** (1) 208-211.

DANEN-LOUWERSE HJ, LIJKLEMA L and COENRAATS M (1995) Co-precipitation of phosphate with calcium carbonate in lake Veluwe. *Water Res.* **29** (7) 1781-1785.

DROOMGOOLE EL and WALTER LM (1990) Iron and manganese incorporation into calcite - Effect of growth kinetics, temperature and solution chemistry. *Chem. Geol*. **81** (4) 311-336.

FERGUSON JF and McCARTY P (1971) Effects of carbonate and magnesium on calcium phosphate precipitation. *Environ. Sci. & Tech.* **5** (6) 534-540.

FRIEND JFC and LOEWENTHAL RE (1992) Chemical Conditioning of Low-and-Medium Salinity Waters Stasoft Version 3.0. Published by the Water Research Commission, South Africa.

GUNN DJ (1976) Mechanisms for the Formation and Growth of Ionic Precipitates from Aqueous Solution. *Far. Discussions of the Chem. Soc.* **61** 133-140.

HOFFMAN RJ and MARAIS GvR (1977) Phosphorus Removal in the Modified Activated Sludge Process. Research Report W22, Dept. of Civil Eng., Univ. of Cape Town, Rondebosch 7701, South Africa.

HOUSE WA (1987) Inhibition of calcite crystal growth by inorganic phosphate. *J. Colloid Interface Sci.* **119** (2) 505-511.

KATEHIS D, DIYAMANDOGLU V and FILLOS J (1998) Stripping and recovery of ammonia from centrate of anaerobically digested biosolids at elevated temperatures. *Water Environ. Research* **70** (2) 231-240.

KOUTSOUKOS P, AMJAD Z, TOMSON MB and NANCOLLAS GH (1980) Crystallization of calcium phosphates: A constant composition study. *J. Am. Chem. Soc.* **27** 1553-1557.

LOEWENTHAL RE, WIECHERS HNS and MARAIS GvR (1986) Softening and Stabilization of Municipal Waters. Published by the Water Research Commission, South Africa.

LOEWENTHAL RE, EKAMA GA and MARAIS GvR (1988) Stasoft - Computer Program for Softening and Stabilisation of Municipal Waters. Published by Water Research Commission, South Africa.

LOEWENTHAL RE, EKAMA GA and MARAIS GvR (1989) Mixed weak acid/base systems: Part I- Mixture characterisation. *Water SA* **15** (1) 3-24.

LOEWENTHAL RE, WENTZEL MC, EKAMA GA and MARAIS GvR (1991) Mixed weak acid/base systems: Part I I- Dosing estimation, aqueous phase. *Water SA* **17** (2) 107-122.

LOEWENTHAL RE, KORNMULLER URC and VAN HEERDEN EP (1994) Struvite precipitation in anaerobic treatment systems. *Water Sci. Technol*. **30** (12) 107-116.

LOEWENTHAL RE and MORISSON IR (1997) Struvite 3.1 - A Calculator for Struvite Precipitation/Dissolution. Dept of Civil Eng., Univ. of Cape Town, Rondebosch 7701, Cape, RSA.

MAMAIS D, PITT PA, CHENG YW, LOIACONO J and JENKINS D (1994) Determination of ferric chloride dose to control struvite precipitation in anaerobic sludge digester. *Water Environ. Res.* **66** (7) 912-918.

MERRILL DT and JORDEN JM (1975) Lime induced reactions in municipal wastewater. *J. WPCF* **47** (12) 2783-2808.

MEYER JL and EANES ED (1978) A thermodynamic analysis of the amorphous to cristalline calcium phosphate transformation. *Calcif. Tiss. Res.* **25** 59-68 (Quoted in Moutin et al., 1992).

MOUTIN T, GAL JY, EL HALOUANI H, PICOT B and BONTOUX J (1992) Decrease of phosphate concentration in a high rate pond by precipitation of calcium phosphate: Theoretical and experimental results. *Water Res.* **26** (11) 1445-1450.

MOHAJIT KK, BHATTARAI E, TAIGANIDES EP and YAP BC (1989) Struvite deposits in pipes and aerators. *Biol. Wastes* **30** 133-147.

MOOSBRUGGER RE, WENTZEL MC, EKAMA GA and MARAIS GvR (1992) Simple Titration Procedures to Determine H_2CO_3* Alkalinity and Short-chain Fatty acids in Aqueous Solutions Containing Known Concentrations of Ammonium, Phosphate and Sulphide Weak Acid/Bases. Published by Water Research Commission, PO Box 824, Pretoria 0001, South Africa.

MUNZ C and ROBERTS P V (1989) Gas and liquid-phase mass transfer resistances of organic compounds during mechanical surface aeration. *Water Res.* **23** (5) 589-601.

MURRAY K and MAY PM (1996) Joint Expert Speciation System (JESS). An International Computer System for Determining Chemical Speciation in Aqueous and Non-aqueous Environments. Murdoch Univ., Murdoch 6150, WA, Australia and the Div. of Water Technol., CSIR, PO Box 395, Pretoria, 0001, South Africa.

MUSVOTO EV, WENTZEL MC, LOEWENTHAL RE and EKAMA GA (1997) Kinetic based model for mixed weak acid/base systems. *Water SA* **23** (4) 311-322.

MUSVOTO EV, WENTZEL MC, EKAMA and LOEWENTHAL RE (1998) Mathematical Modelling of Integrated Chemical, Physical and Biological Treatment of Wastewaters. Research Report W97, Univ. of Cape Town, Dept. of Civil Eng. Rondebosch 7701, Cape, South Africa.

MUSVOTO EV, WENTZEL MC and EKAMA GA (2000) Integrated chemical-physical processes modelling Part II - Simulating aeration

treatment of anaerobic digester supernatants. *Water Res.***34** (6) 1868-1880.

NORDSTROM DK, PLUMMER NL, LANGMUIR D, BUSENBERG E, MAY HM, JONES BF and PARKHURST DL (1990) Revised chemical and equilibrium data for major water-mineral reactions and their limitations. *Am. Chem. Soc.* **416** 398-413.

PITMAN AR, DEACON SL, ALEXANDER WV, NICHOLLS HA, BOYD R SA and MINSON D (1989) New methods for conditioning and dewatering sewage sludges in Johannesburg. *Proc. WISA 1st Biennial Conf. & Exhib.*, Cape Town, South Africa.

PITMAN AR (1999) Management of biological nutrient removal plant sludges - Change the paradigms? *Water Res.* **33** (5) 1141-1146.

REICHERT P (1994) *Concepts Underlying a Computer Program for the Identification and Simulation of Aquatic Systems*. Swiss Federal Institute for Environmental Science and Technology (EAWAG). CH-8600 Dübendorf. Switzerland.

ROQUES H and GIROU A (1974) Kinetics of the formation conditions of carbonate tartars. *Water Res.* **8** (11) 907-920.

SCOTT WD, WRIGLEY TJ and WEBB KM (1991) A computer model for struvite solution chemistry. *Talanta* **38** (8) 889-895.

SILLEN LG and MARTELL AE (1964) *Stability Constants of Metal Ion Complexes*. Special publications, The Chemical Society, London.

STANDARD METHODS (1985) *Standard Methods for the Examination of Water and Wastewater* (16th edn.) APHA, AWWA & WPCF, New York.

STRATFUL I, BRETT S, SCRIMSHAW MB and LESTER JN (1999) Biological phosphorus removal, its role in phosphorus recycle. *Environ. Technol.* **20** (7) 681-695.

STUMM W and MORGAN JJ (1981) *Aquatic Chemistry: An Introduction Emphasizing Chemical Equilibria in Natural Waters*. Wiley-Interscience, New York.

TAYLOR AW, FRAZIER AW and GURNEY E L (1963) *Trans. Faraday Soc.* **59** 1580.

VERBEECK RHM and DEVENYNS JAH (1992) The kinetics of dissolution of octacalcium phosphate II. The combined effects of pH and solution Ca/P ratio. *J. Cryst. Growth* **121** 335-338.

WIECHERS HNS, LOEWENTHAL RE and MARAIS GvR (1980) Lime treatment of wastewater: Development and application of a simple graphical technique for predicting the chemical composition of lime-treated secondary effluent. *Prog. Water Technol.* **12** (Toronto) 347-358.

WILLIAMS S (1999) Struvite precipitation in the sludge stream at slough wastewater treatment plant and opportunities for phosphorus recovery. *Environ. Technol.* **20** (7) 743-747.

WOODS NC, SOCK SM and DAIGGER GT (1999) Phosphorus recovery technology modelling and feasibility evaluation for municipal wastewater treatment plants. *Environ. Technol.* **20** (7) 663-679.